



## Adsorption of heavy metals by activated carbon: effect of natural organic matter and regeneration methods of the adsorbent

Lijia Qiu<sup>a</sup>, Chengyu Suo<sup>a</sup>, Nannan Zhang<sup>b</sup>, Rongfang Yuan<sup>a,\*</sup>, Huilun Chen<sup>a</sup>, Beihai Zhou<sup>a,\*</sup>

<sup>a</sup>Beijing Key Laboratory of Resource-Oriented Treatment of Industrial Pollutants, Department of Environmental Science and Engineering, School of Energy and Environmental Engineering, University of Science and Technology Beijing, Beijing 100083, China, emails: yuanrongfang@ustb.edu.cn (R. Yuan), zhoubeihai@sina.com (B. Zhou), qiulj0221@163.com (L. Qiu), 1142728357@qq.com (C. Suo), chenhuilun@ustb.edu.cn (H. Chen)

<sup>b</sup>Water Reclamation Plant at Future Sci-Tech City, Changping District of Beijing Water Authority, Beijing 102209, China, email: znn1103@163.com

Received 30 August 2021; Accepted 8 January 2022

### ABSTRACT

At present, global water resources are seriously polluted by heavy metals. It is necessary to take timely measures to remove heavy metals from wastewater. In this study, the effect of natural organic matter (NOM) on the adsorption of heavy metals by activated carbon was confirmed, and the optimal regeneration method of activated carbon was obtained. The results showed that the order of adsorption capacities of activated carbon for five heavy metals was Cu(II) > Cr(VI) > Pb(II) > Zn(II) > Cd(II). NOM, which is widely present in wastewater, affected the adsorption capacities of heavy metals. The equilibrium adsorption capacities of activated carbon for Pb(II), Zn(II), Cd(II) and Cu(II) increased by 0.031, 0.023, 0.001 and 0.012 mmol/g respectively, while the equilibrium adsorption capacity for Cr(VI) decreased by 0.020 mmol/g when the concentration of NOM was 1 mg/L. With the raise of NOM concentration, the promoting effect of NOM on the removal of Pb(II) and Zn(II) was gradually reduced, and the promoting degree of Cd(II) adsorption and the inhibiting degree of Cr(VI) adsorption were correspondingly enhanced. At the same time, the influence of high concentration of NOM on the removal of Cu(II) was changed from promotion to inhibition. In addition, HCl solution of 0.1 mol/L was confirmed to be the best regeneration reagent for desorbing metal ions on activated carbon through regeneration experiments. After six adsorption–regeneration cycles, the high adsorption performance of activated carbon could still be maintained.

*Keywords:* Activated carbon; Heavy metal; Adsorption; Natural organic matter; Regeneration

### 1. Introduction

With the rapid development of electroplating, textile, mining, tanning and other industries in the past decades, water pollution caused by heavy metals has been regarded as a serious environmental problem threatening the world [1–3]. Although trace amounts of several heavy metals can be absorbed by organisms as daily supplements, heavy metals

are stubborn and persistent, and are not easy to be biodegraded. When heavy metals in water gradually accumulate to an excessive amount, the surrounding environment, animals and plants, and human health will be seriously damaged [4–6]. Consequently, heavy metals in wastewater need to be removed.

A variety of technologies, including chemical precipitation, adsorption, ion exchange, membrane filtration and electrolysis, have been used for the treatment of wastewater

\* Corresponding authors.

polluted by heavy metals [7,8]. However, metal sludge is prone to be produced in the process of chemical precipitation, which causes the sludge treatment load to be increased [9]. When ion exchange is selected to remove heavy metals, the resins are easily to be contaminated or oxidized. Membrane filtration technologies, such as ultrafiltration and reverse osmosis, usually have relatively high investment and operating costs. In addition, backwashing is constantly required during the filtration process, which leads to complicated operations. The main disadvantages of electrolysis, which make it difficult to be widely promoted and applied, are high power consumption and short service life of electrode materials [10]. Adsorption is a method that porous solid materials are used to adsorb heavy metals in wastewater. Compared with other technologies, many promising characteristics are possessed by adsorption, including simple operation, small footprint, stable effect, low cost and regeneration potential [11,12]. Among adsorbents, considerable attention and application have been received for activated carbon [13,14].

As an adsorption material, activated carbon has good porosity, large specific surface area, and abundant functional groups on the surface and inside [15]. The excellent adsorption performance for heavy metals is produced by these characteristics. Therefore, activated carbon has been widely studied due to low price and stable removal effect of heavy metals [16–18]. As an example, it had been reported that Pb(II), Co(II) and Ni(II) in wastewater could be removed by more than 97.54% when activated carbon made from lemon leaves was used [19]. By comparing the adsorption effects of activated carbon on Pb(II) and Cr(VI) before and after modification, a recent study indicated that the adsorptive property of activated carbon for heavy metals could be enhanced by thermal tension method [20].

However, the adsorption of heavy metals is easily affected by other substances in wastewater [21], especially natural organic matter (NOM). NOM is ubiquitous in the water system such as industrial wastewater, domestic sewage and surface water [22]. It has complex ingredients and can weaken the adsorption capacities of activated carbon on heavy metals by competing for adsorption sites and blocking pores [23]. Research demonstrated that metal ions can also be combined by NOM to form coordination compounds [24]. For these reasons, the inhibitory or promoting effect of NOM on the adsorption of heavy metals by activated carbon needs to be determined by study. Moreover, when multiple heavy metals are present in wastewater at the same time, the influence of NOM on the adsorption effect is not yet clear.

Furthermore, in the actual application process, the regeneration and recycling of the saturated activated carbon need to be considered in order to reduce the treatment cost and control the secondary pollution of the water environment caused by adsorbent [25]. Although there are many regeneration methods, including electrochemistry, biological process, heat treatment and microwave method, the effect of chemical regeneration is proved to be the best for activated carbon which adsorbed heavy metals [26–29]. However, the chemical reagents for simultaneous desorption of various metal ions on activated carbon have not been studied by previous researchers.

The objective of this research was to determine the influence of NOM on the adsorption of different heavy metals

by activated carbon, and to obtain the optimal regeneration method after activated carbon adsorption. Pb(II), Cu(II), Zn(II), Cd(II) and Cr(VI) were selected as research objects. Different concentrations of NOM were added to explore the inhibitory or promoting effect of heavy metals adsorption through adsorption kinetics study, Brunauer–Emmett–Teller (BET) and scanning electron microscope (SEM) detection. Then, the types and concentrations of activated carbon regenerated reagents, and the regeneration times of activated carbon were investigated.

## 2. Materials and methods

### 2.1. Materials

Wooden granular activated carbon was purchased from Yiqing activated carbon Co., Ltd., (Jiangsu, China). Activated carbon used in this study was immersed and washed in deionized water for several times to remove dust and impurities. After drying, the activated carbon was sieved into 0.15 mm particles.  $\text{Pb}(\text{NO}_3)_2$ ,  $\text{Cu}(\text{NO}_3)_2 \cdot 3\text{H}_2\text{O}$ ,  $\text{Zn}(\text{NO}_3)_2 \cdot 6\text{H}_2\text{O}$ ,  $\text{Cd}(\text{NO}_3)_2 \cdot 4\text{H}_2\text{O}$ ,  $\text{K}_2\text{Cr}_2\text{O}_7$ , NaCl, HCl and NaOH with analytical reagent grade were obtained from Sinopharm Chemical Reagent Co., Ltd. (Shanghai, China). NOM was obtained from International Humic Substances Society (IHSS). In addition, deionized water (resistivity > 18 M $\Omega$  cm) for preparing the solutions required in the experiments was provided by a Milli-Q System (USA).

### 2.2. Experimental procedures

#### 2.2.1. Adsorption of heavy metals

In a previous study [30], the dosage of 0.8 g/L activated carbon was proved to be more reasonable considering the removal effect and economic cost. Therefore, activated carbon of 0.8 g/L was used to remove heavy metals. Single heavy metal solution of Pb(II), Cu(II), Zn(II), Cd(II) or Cr(VI) with initial concentration of 0.5 mmol/L was prepared. The adsorption experiments were carried out in a thermostatic oscillator after activated carbon was added into the solutions. The oscillator speed and reaction temperature were set at 250 rpm and 25°C, respectively. Water samples were obtained at different contact times (0–240 min), and then immediately filtered through a 0.45  $\mu\text{m}$  filter membrane. The concentration of residual heavy metals in water samples after adsorption was determined.

#### 2.2.2. Influence of NOM

In order to explore the influence of different concentrations of NOM on the adsorption of heavy metals, mixed solutions of single heavy metal (Pb(II), Cu(II), Zn(II), Cd(II) or Cr(VI)) and NOM were prepared, respectively. The concentration of each heavy metal was 0.5 mmol/L. The concentration of NOM was adjusted to 0, 1, 5 or 10 mg/L, and then the numbers of water samples can be defined as heavy metal-0, heavy metal-1, heavy metal-5 and heavy metal-10. Activated carbon of 0.8 g/L was used to adsorb the mixed solution of single heavy metal and NOM in an oscillator at 25°C and 250 rpm. The amounts of heavy metals adsorbed under different contact time were analyzed and the kinetic

models were fitted. In order to evaluate the effect of temperature on adsorption effect, thermodynamic studies with NOM of 0 and 10 mg/L were carried out, with temperature gradients of 15°C, 25°C, 35°C, 45°C and 55°C. The nature of adsorption process of activated carbon for heavy metals was clarified by the Gibbs free energy ( $\Delta G$ ), variation of enthalpy ( $\Delta H$ ) and variation of entropy ( $\Delta S$ ) obtained.

Under the conditions of NOM of 0 and 10 mg/L, the activated carbon in the solution was separated by pressure filtration. The activated carbon with neutral pH value was obtained after repeated washing with deionized water, and then the drying oven was used for constant temperature drying. The specific surface area,  $N_2$  adsorption–desorption isotherm, pore-size distribution and surface morphology of activated carbon were analyzed, and the functional groups of activated carbon and NOM were studied.

### 2.2.3. Activated carbon regeneration

The adsorption activated carbon obtained through pressing, rinsing and drying was stirred with deionized water ( $H_2O$ ), or NaCl, HCl or NaOH solution of 0.1 mol/L, respectively. The concentration of heavy metals was detected, and the desorption rate of activated carbon was determined.

HCl solutions with concentrations of 0.01, 0.05, 0.1, 0.2, 0.5 and 1 mol/L were prepared for desorption and regeneration of activated carbon after adsorption equilibrium. The desorption rates of activated carbon at different HCl concentrations were compared. Then 0.5 mmol/L Pb(II), Cu(II), Zn(II), Cd(II) and Cr(VI) solutions were adsorbed on regenerated activated carbon. The removal rate of heavy metals was calculated. The optimal concentration of HCl solution was chosen for repeated adsorption–desorption treatment of activated carbon, and the influence of regeneration times was analyzed.

### 2.2.4. Description of employed equations

Table 1 shows all equations employed in the current research.

### 2.3. Analytical methods

The concentration of heavy metals in the solution was determined by inductively coupled plasma optical emission spectrometer (ICP-OES, iCAP 7000 Plus series, USA). The functional groups of activated carbon and NOM were analyzed by Fourier-transform infrared spectrometer (FT-IR

Table 1  
Basic equations and mathematical models used for kinetic and thermodynamic studies

Basic equations		
Amount of adsorption	$q_t = \frac{(C_0 - C_t)V}{m}$	$q_t$ (mmol/g): amount of each metal adsorbed by activated carbon at time $t$ (min); $C_0$ (mmol/L): initial concentration of heavy metals; $C_t$ (mmol/L): concentration of heavy metals at time $t$ (min); $V$ (L): volume of aqueous phase; $m$ (g): mass of activated carbon.
Desorption rate	$D_p = \frac{C_2 V_2}{(C_0 - C_1) V_1} \times 100\%$	$D_p$ (%): desorption rate of activated carbon; $C_0$ (mmol/L); $C_1$ (mmol/L): initial and equilibrium concentrations of heavy metals, respectively; $C_2$ (mmol/L): heavy metals concentration of regeneration solution after desorption, $V_1$ (L): volume of adsorption solution; $V_2$ (L): volume of regeneration solution;
Removal rate	$R = \frac{(C_0 - C_1)}{C_0} \times 100\%$	$R$ (%): removal rate of heavy metals by activated carbon.
BET [31]	$\frac{1}{v \left[ \frac{p_0}{p} - 1 \right]} = \frac{c-1}{v_m c} \left( \frac{p}{p_0} \right) + \frac{1}{v_m c}$	$p$ (Pa) and $p_0$ (Pa): equilibrium and saturation pressures of activated carbon at the adsorption temperature, respectively; $v$ (mL): amount of adsorbed gas; $v_m$ (mL): amount of adsorbed gas in monolayer; $c$ : constant of BET.
Kinetic nonlinear models		
Pseudo-first-order	$q_t = q_e (1 - e^{-k_1 t})$	$q_t$ (mmol/g) and $q_e$ (mmol/g): amounts of heavy metals adsorbed at time $t$ (min) and at equilibrium, respectively; $k_1$ (1/min) and $k_2$ (g/(mmol min)):
Pseudo-second-order [32,33]	$q_t = \frac{k_2 q_e^2 t}{1 + k_2 q_e t}$	rate constants for pseudo-first-order and pseudo-second-order adsorption models, respectively.
Intraparticle diffusion (linear) [34]	$q_t = k_i t^{0.5} + d$ $D_i = \frac{0.03 r^2}{t^{0.5}}$	$k_i$ (mmol/(g min <sup>0.5</sup> )): rate constant for intraparticle diffusion model; $d$ (mmol/g): effect of boundary layer thickness; $D_i$ (cm <sup>2</sup> /s): intraparticle diffusion coefficient; $r$ (cm): average pore radio.
Thermodynamic linear models		
Gibbs free energy parameter	$\Delta G = -RT \ln K_d$	$K_d$ : ratio of the amount adsorbed per unit of activated carbon ( $q_e$ ) and solution concentration in equilibrium ( $C_e$ ); $R$ : universal gas constant (8.314 J/(mol K));
Enthalpy and entropy parameters [35]	$\ln K_d = \frac{\Delta S}{R} - \frac{\Delta H}{RT}$	$T$ (K): experimental temperature. The values of $\Delta H$ and $\Delta S$ were obtained from the graph of $\ln K_d$ in function of $1/T$ .

Spectrometer, Perkin Elmer Frontier, Japan) in transmission mode using KBr pellets. The detection area was between 400 and 4,000  $\text{cm}^{-1}$  and the resolution was 4  $\text{cm}^{-1}$ . The specific surface area,  $\text{N}_2$  adsorption–desorption isotherm and pore-size distribution curve of activated carbon, based on the famous BET theory, were obtained by specific surface area and porosity analyzer (ASAP 2020M, USA). The distribution of heavy metals and NOM on the surface and pores of activated carbon could be directly reflected by the surface morphology of activated carbon before and after adsorption, which was observed using scanning electron microscope (SEM, S-4800, Japan). All experiments were repeated twice to control the errors.

### 3. Results and discussions

#### 3.1. Adsorption effect of activated carbon on heavy metals

In order to reveal the adsorption effect of activated carbon on different heavy metals, the changes of the amounts of Pb(II), Cu(II), Zn(II), Cd(II) and Cr(VI) adsorbed under different contact time were studied. The results are shown in Fig. 1.

It can be seen that the adsorption was relatively rapid in the first few minutes. About 75% of the equilibrium adsorption capacities for five heavy metals were obtained within 2 min. Then, the amounts of adsorption increased slowly with the increase of time, indicating the removal rates of heavy metals decreased. The dynamic equilibrium stage of Pb(II), Zn(II) and Cd(II) was reached at 30 min, while the equilibrium time of Cu(II) and Cr(VI) was longer, and the maximum amount of adsorption was not achieved at 240 min. Therefore, the reaction process between activated carbon and heavy metals was divided into two stages, that is, a former rapid step and a subsequent slow step, which was consistent with the observation of other researchers [36,37]. In the initial contact process, the adsorption sites on the surface of activated carbon were sufficient, and the heavy metals were quickly removed by physical and chemical adsorption. Afterwards, the available active sites gradually

decreased, resulting in the amounts of metals adsorbed slowly increasing to a stable state.

As shown in Fig. 1, the adsorption capacities of activated carbon for five heavy metals were different, the adsorption capacity of Cu(II) (0.144 mmol/g) was the largest, while that of Cd(II) (0.040 mmol/g) was the least.  $\text{Cu(II)} > \text{Cr(VI)} > \text{Pb(II)} > \text{Zn(II)} > \text{Cd(II)}$  was determined to be the order of adsorption capacities of five heavy metals, which is mainly related to the characteristics of different metal ions, such as ionic radius, hydration heat and electronegativity [38]. The ionic radii of Cu(II), Cr(VI), Pb(II), Zn(II) and Cd(II) are 0.72, 0.52, 1.20, 0.74 and 0.97 Å, respectively. The pores of activated carbon would be overcrowded and blocked by ions with larger radius, and the adsorption sites could not be fully utilized [39]. Thus, metal ions with smaller radius, such as Cu(II) and Cr(VI), were easily removed by activated carbon. Although the largest ionic radius of Pb(II) was observed, the hydration heat of Pb(II) was lower than that of Zn(II). The low hydration heat could make the complex water easy to be removed, and the generated bare Pb(II) had a strong ability to exchange with cations on the surface or inside of the adsorbent [40,41]. Furthermore, the relative electronegativities of Cu(II), Cr(VI), Pb(II), Zn(II) and Cd(II) are found to be 1.9, 1.6, 1.9, 1.6 and 1.7. The comparison shows that Pb(II) and Cu(II) have the highest electronegativity and the strongest ability to attract electrons [42], and the covalent bonds with oxygen-containing groups of activated carbon are also easily formed. These are the reasons why the amount of Pb(II) adsorbed by activated carbon was higher than that of Zn(II) and Cd(II), and the adsorption capacity of Cu(II) was higher than that of Cr(VI). Moreover, the complexation reaction could be occurred between the active center ( $-\text{OH}$ ) of the adsorbent and Cu(II) [43], and the solubility product of  $\text{Cu(OH)}_2$  produced was detected to be low, which indicated that it was difficult to dissolve in water. Comprehensive analysis shows that the strongest adsorption capacity of activated carbon for Cu(II) was mainly due to the smaller ionic radius and solubility product of precipitated product, and the largest electronegativity.

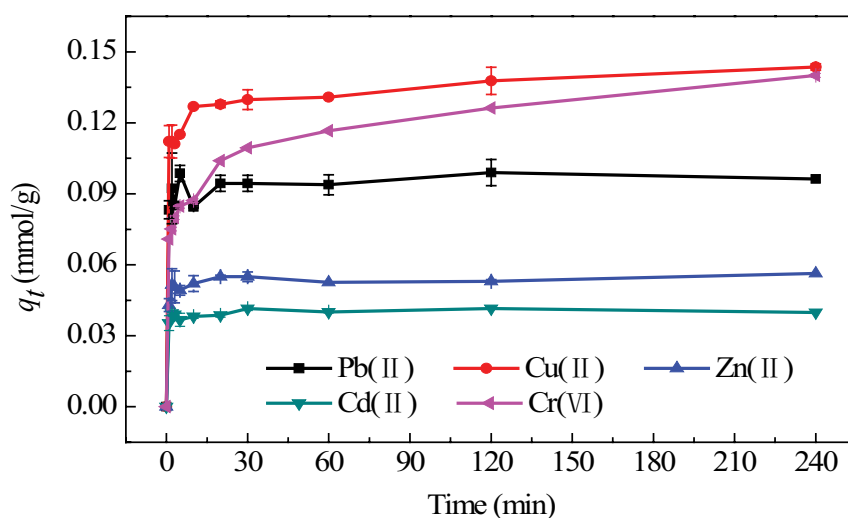


Fig. 1. The amounts of different heavy metals adsorbed by activated carbon.

### 3.2. Effect of NOM on adsorption of heavy metals

#### 3.2.1. Functional groups of the adsorbent and NOM

The chemical adsorption property of activated carbon is determined by the surface chemistry, and functional group is an important part of the chemical property. A large number of functional groups will be provided by NOM which is widely present in water, so the adsorption effect of activated carbon on heavy metals will be affected. Therefore, the functional groups of activated carbon and NOM were focused on analysis, and the detection results are shown in Fig. 2.

Common wooden granular activated carbon was the adsorbent used in this research, which has abundant pores, large specific surface area and strong adsorption capacity. The chemical adsorption capacity of activated carbon depends on the abundant functional groups on the surface and inside of the particles. It can be seen from Fig. 2a that the infrared characteristic vibrational peaks of activated carbon were obtained in regions of 588–671  $\text{cm}^{-1}$ , 1,105–1,260  $\text{cm}^{-1}$ , 1,383–1,436  $\text{cm}^{-1}$ , 1,628  $\text{cm}^{-1}$ , 2,850 to 2,931  $\text{cm}^{-1}$  and 3,432  $\text{cm}^{-1}$ . As already mentioned, the peaks observed between 588 and 671  $\text{cm}^{-1}$  were attributed to the out-of-plane bending vibration of C–H bonds in chain olefins, while

the activated carbon contained alcohols and phenols (C–O bonds) [44], and the existence of C–O–P phosphorus-containing functional groups was proved by absorption peaks at 1,105–1,260  $\text{cm}^{-1}$ . Moderate absorption was detected in the range of 1,383–1,436  $\text{cm}^{-1}$ , indicating that the nitrogen in the activated carbon composition was mainly in the form of N–H [45]. According to the division of the infrared spectrum, 1,500–2,000  $\text{cm}^{-1}$  should belong to the vibrational stretching of the double bonds, so the absorption peak at 1,628  $\text{cm}^{-1}$  was mainly related to the C=C and C=O groups in the aromatic ring, lactone and anhydride [46]. This may be because activated carbon underwent dehydration and cleavage reactions through high temperature activation, thereby forming double bonds. The reducibility of activated carbon could be enhanced by the C=C bonds, and part of the negative charge on the surface of the adsorbent was generated by the C=O bonds of the carboxyl groups. The hydrogen-containing functional groups were mainly reflected in the range of 2,500–4,000  $\text{cm}^{-1}$ , including the asymmetric vibration of methylene C–H, and the stretching vibration of O–H in alcohol and phenol [47]. In summary, there were a large number of functional groups in activated carbon, such as C–O, COO<sup>-</sup>, O–H bonds, which were conducive to the adsorption of heavy metals.

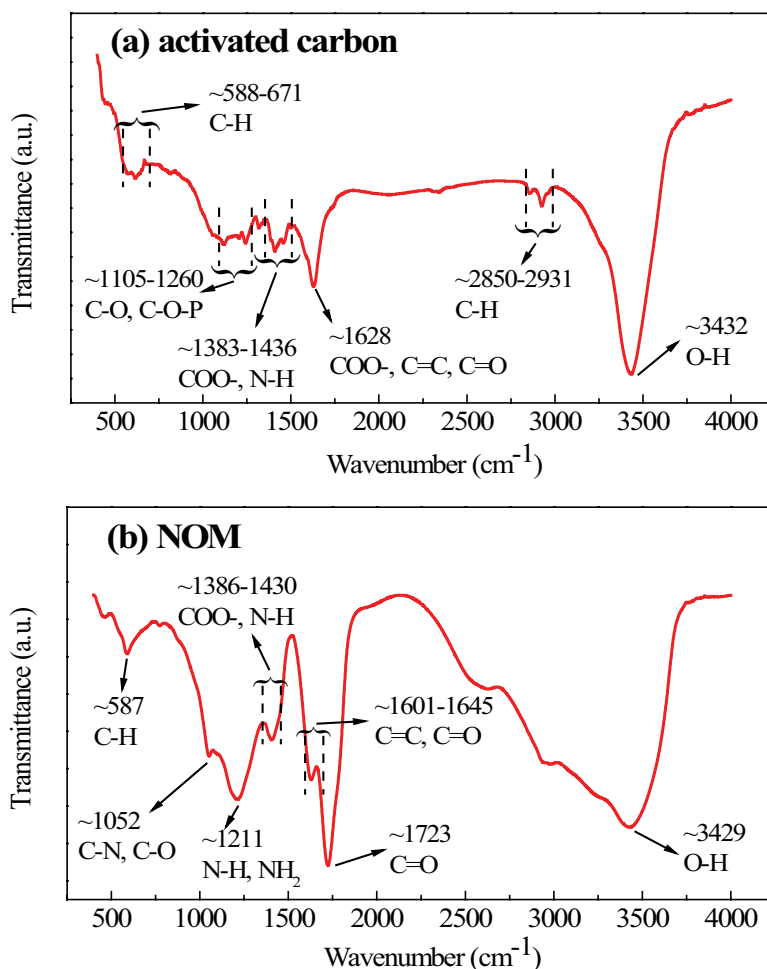


Fig. 2. FT-IR from 400 to 4,000  $\text{cm}^{-1}$  for activated carbon and NOM.

NOM in water was a kind of complex organic substance mixture. Humus, such as fulvic acid and humic acid, was the most important component of NOM, which accounted for about 60%–90% of NOM content. In addition, a small amount of polysaccharides, proteins and hydrophilic organic acids were detected in NOM. The NOM used in this study was provided by the International Humic Substances Society (IHSS), which was called Suwannee River NOM. The test showed that Suwannee River NOM was mainly composed of C (50.70%), H (3.97%), O (41.48%), N (1.27%), and S (1.78%). FT-IR was used to analyze the functional groups of Suwannee River NOM, and the results are shown in Fig. 2b. Vibrational stretching was observed at 587  $\text{cm}^{-1}$ , 1,052  $\text{cm}^{-1}$ , 1,211  $\text{cm}^{-1}$ , 1,386 to 1,430  $\text{cm}^{-1}$ , 1,601 to 1,645  $\text{cm}^{-1}$ , 1,723  $\text{cm}^{-1}$  and 3,429  $\text{cm}^{-1}$ , which were attributed to the presence of C–H, C–N, C–O, N–H,  $\text{NH}_2$ ,  $\text{COO}^-$ , N–H, C=C, C=O and O–H bonds in NOM, respectively [48]. When there was a large amount of NOM in water, some new functional groups, such as O–H,  $\text{COO}^-$  and C=O, were introduced by NOM, which could provide more adsorption sites for heavy metals in water and combine with metal ions to form coordination compounds, so that the removal effect of heavy metals in polluted water was enhanced.

### 3.2.2. Adsorption kinetics under the influence of different concentrations of NOM

The adsorption kinetics of Pb(II), Cu(II), Zn(II), Cd(II) and Cr(VI) by activated carbon with different concentrations of NOM were studied. The pseudo-first-order kinetic, pseudo-second-order kinetic and intraparticle diffusion models are important indicators to characterize the reaction rate and adsorption process, so these typical models were used for evaluation in the experiment.

The fitting images of Pb(II) by the three kinetic models under different NOM concentrations are shown in Fig. 3, and the fitting parameters are listed in Table S1. It can be seen from the fitting images that the adsorption reaction mainly was occurred in the first few minutes of contact, and the reaction rate was relatively large. Subsequently, the amount of adsorption was detected to increase slowly and the reaction rate decreased. This response trend was not changed by the presence of NOM in wastewater. The pseudo-first-order model is based on the linear relation between the adsorption rate and the number of active sites, while the pseudo-second-order model is defined as the linear relation between the reaction rate and the square of the number of active sites. The adsorption process is better explained by both models. Considering high values of adjusted determination coefficient ( $\text{Adj-}R^2$ ), low values of standard deviation ( $\sigma$ ), and proximity of the quantities adsorbed in equilibrium ( $q_{e(\text{cal.})}$ ) to that experimentally obtained ( $q_{e(\text{exp.})}$ ) [31], the fitting degree of pseudo-second-order equation was relatively better than that of pseudo-first-order equation, suggesting the process of removing heavy metals by activated carbon was mainly controlled by the chemical force through the secondary adsorption rate. Similar conclusions had been found by other researchers [49–51].

However, the adsorption mechanism cannot be fully explained by pseudo-second-order kinetic, so intraparticle diffusion (Weber–Morris) model needs to be used for

multilinear analysis. According to the parameters of Weber–Morris model in Table S1, although only some values of  $\text{Adj-}R^2$  were close to 1, the values of  $\sigma$  were small, and the calculated adsorption capacities ( $d$ ) and the experimental  $q_{e(\text{exp.})}$  were close to each other, indicating the partial removal of Pb(II) by activated carbon was controlled by intraparticle diffusion [45]. By observing Fig. 3e and f, it was found that the process of heavy metals adsorption on activated carbon particles was mainly divided into three phases. In the first minute of adsorption, Pb(II) was first transferred from water to the surface of liquid membrane formed around activated carbon due to hydration. In the second-phase, Pb(II) overcame the resistance and passed through the liquid membrane to reach and be adsorbed on the surface active sites of activated carbon. The bonding strength was determined by whether the process was a physical or chemical effect. In the third phase, Pb(II) was diffused and adsorbed to the inside of activated carbon particles [47,48]. When the concentrations of NOM in water were different, the differences of intraparticle diffusion coefficient ( $D$ ) were small, which were all within the range of  $10^{-5}$  to  $10^{-13}$   $\text{cm}^2/\text{s}$ , indicating the removal rate of heavy metals could be limited by the diffusion rate in the particles, and the degree of restriction was more significant in the chemical adsorption process [52].

Comparing with the fitting parameters of pseudo-second-order model in Table S1, the equilibrium adsorption capacity of 0.095 mmol/g for Pb(II) was achieved when there was no NOM in water, while the equilibrium adsorption amount increased to 0.126 mmol/g with NOM concentration of 1 mg/L. This was mainly because NOM in wastewater has multiple functional groups, such as O–H,  $\text{COO}^-$  and N–H, which could react with metal ions to form coordination compounds [53]. The stability of Pb(II)-NOM coordination compound was proved to be relatively strong in the products formed. Also, most of NOM are anionic polymer organic matters. Pb(II) had the largest ionic radius (1.20 Å) among the five heavy metals, and the micropores of activated carbon were easily blocked by it. Therefore, Pb(II) could be better adsorbed and removed under the help of NOM with high molecular weight because new adsorption sites for Pb(II) were provided when NOM was added. However, the competition ability of NOM for the active sites of adsorbent was enhanced with the raise of NOM concentration [54]. Moreover, high concentration of NOM was easy to block the pores and wrap the surface of activated carbon, which meant that the effective contact area between heavy metals and activated carbon was reduced [54]. Combining the promotion and inhibition effects of NOM on adsorption, these are the main reasons why the adsorption capacities of activated carbon for Pb(II) were ranked as  $\text{Pb(II)-1} > \text{Pb(II)-5} > \text{Pb(II)-10} > \text{Pb(II)-0}$ .

According to the experimental results of Pb(II), the kinetic curve of activated carbon adsorbing heavy metals was more in line with the pseudo-second-order model. Thus, the adsorption procedures of Cu(II), Zn(II), Cd(II) and Cr(VI) under different NOM concentrations were fitted by this model, and the fitting images and parameters are shown in Fig. 4 and Table S2. Research suggested that the influences of different concentrations of NOM on several heavy metals were diverse from each other, which mainly depended on the metal properties such as the affinity of

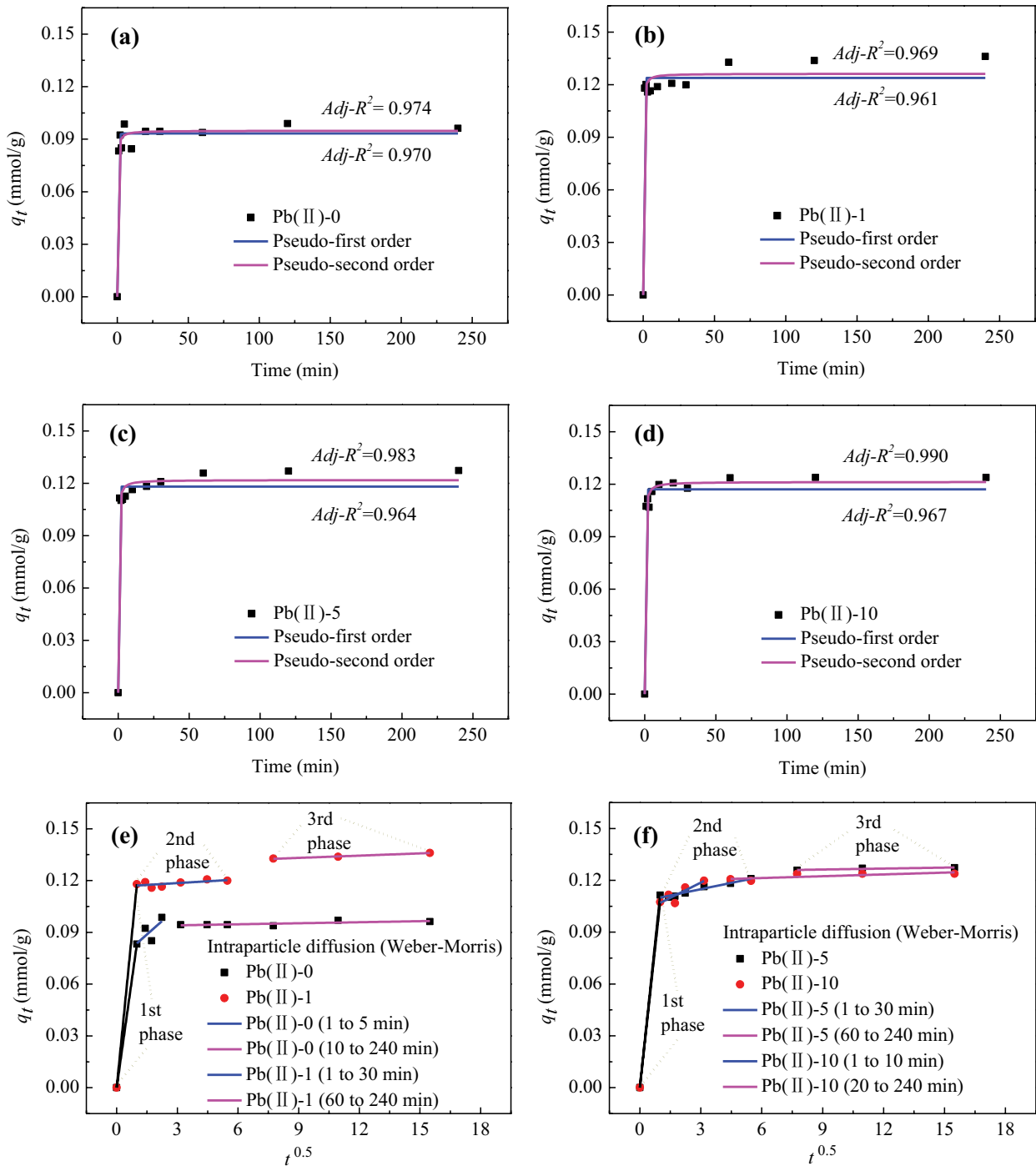


Fig. 3. Adsorption kinetics for Pb(II) at different NOM concentrations (Pb(II)-0: NOM = 0 mg/L, Pb(II)-1: NOM = 1 mg/L, Pb(II)-5: NOM = 5 mg/L, Pb(II)-10: NOM = 10 mg/L).

heavy metals and NOM, ionic radius, electronegativity and complex stability.

From the pseudo-second-order kinetic simulation results of Cu(II), the adsorption of Cu(II) was promoted under the help of 1 mg/L NOM, and the adsorption capacity increased from 0.132 to 0.144 mmol/g, while the adsorption capacity of activated carbon was inhibited by competition of adsorption sites and blockage of pores when 5

or 10 mg/L NOM was added. In other words, the equilibrium adsorption amounts of Cu(II) were in the order of Cu(II)-1 > Cu(II)-0 > Cu(II)-5 > Cu(II)-10. Comparing the influence of NOM on the removal of Cu(II) and Pb(II), the amount of Pb(II) adsorbed increased by 27% and that of Cu(II) decreased by 11% when there was 10 mg/L NOM in water. That was, high concentration of NOM promoted the removal of Pb(II), but inhibited the adsorption of Cu(II),



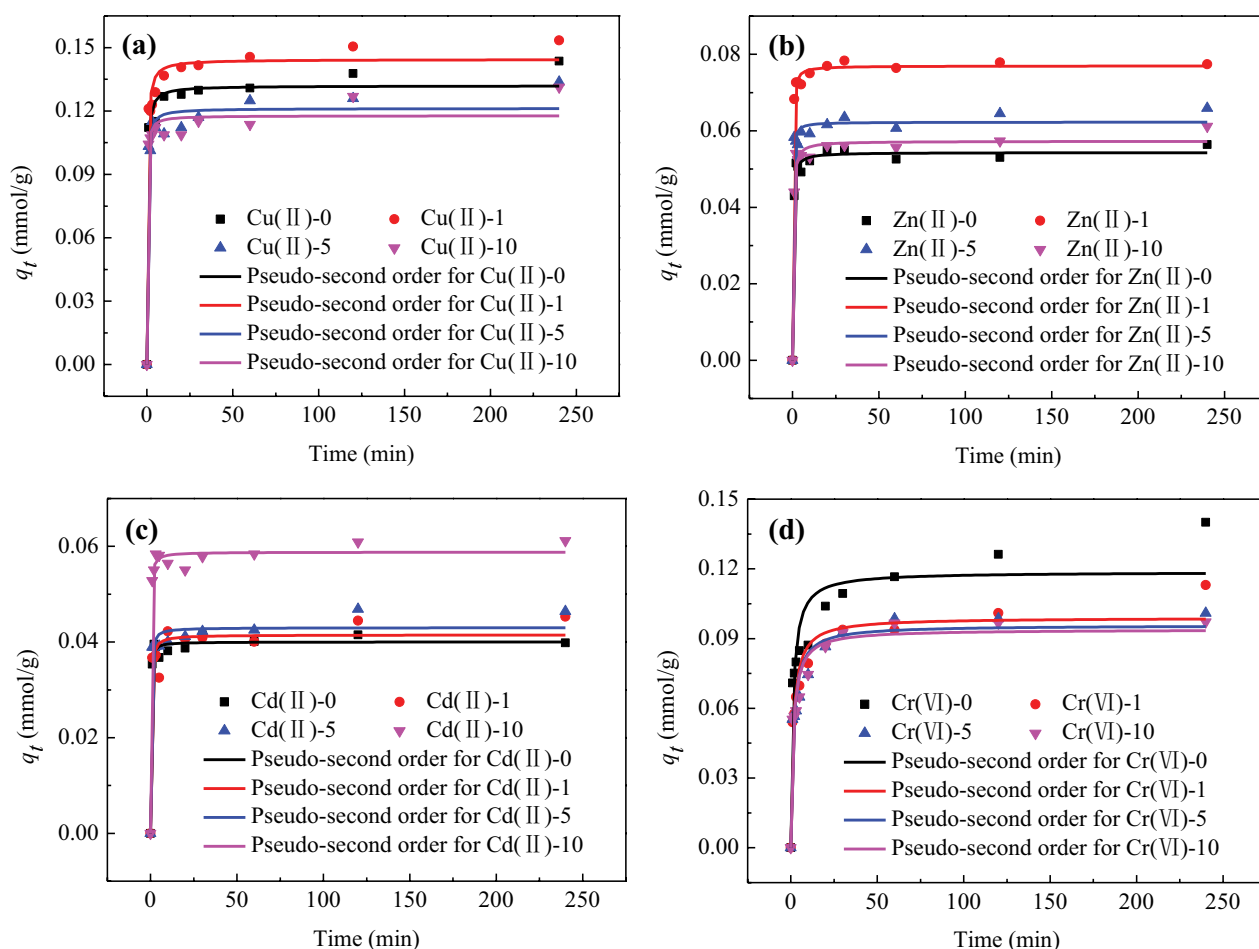


Fig. 4. Pseudo-second-order fitting for Cu(II), Zn(II), Cd(II) and Cr(VI) at different NOM concentrations.

which should be attributed to the different stability of complexes of heavy metals with NOM. Previous studies [55] have shown that Cu(II) had the highest affinity for NOM among the five heavy metals, and the stability of Cu(II)-humic acid complex was much stronger than that of Pb(II)-humic acid complex. Consequently, with the increase of NOM, Cu(II) could not only be adsorbed by the NOM on the surface of activated carbon, but also be attached to the humic acid suspended in wastewater in a large amount, which caused the adsorption of Cu(II) on activated carbon to be prevented [56].

Observing the pseudo-second-order kinetic parameters of Zn(II), the equilibrium adsorption capacities order of Zn(II)-1 > Zn(II)-5 > Zn(II)-10 > Zn(II)-0 was obtained, which was consistent with the order of Pb(II). Even though the hydration heat of Zn(II) was higher than that of Pb(II), which made the ion exchange between Zn(II) and the cations in NOM and activated carbon difficult to be realized [40], the ionic radius of Zn(II) was smaller than that of Pb(II), meaning that Zn(II) was easier to diffuse into the interior of NOM and activated carbon, and the effective specific surface area of adsorbent was relatively larger. Also, the hydroxyl groups in humic acid could react with metal ions, and the solubility product of Zn(OH)<sub>2</sub> ( $1.2 \times 10^{-17}$ ) was less than that of Pb(OH)<sub>2</sub> ( $1.2 \times 10^{-15}$ ), demonstrating that Zn(OH)<sub>2</sub> was more likely to be precipitated, and the possibility of Zn(II) removal

by NOM was greater. As a result, although the active sites of activated carbon were occupied by NOM, the removal efficiency of Zn(II) could be enhanced by the formation of activated carbon-NOM-Zn(II) ternary compounds.

Similarly, the ionic radius of Cd(II) was smaller than that of Pb(II), and the possibility of Cd(II) being transferred to the pores of NOM was stronger than that of Pb(II). This resulted in Cd(II) being favorably removed under the help of NOM. From the previous research results, it was known that the adsorption capacity of activated carbon for Cd(II) was the weakest among the five heavy metals, but the removal effect of Cd(II) may be enhanced by the functional groups of humic acid. Hence the equilibrium adsorption amount of Cd(II) gradually increased from 0.040 to 0.059 mmol/g with the raise of NOM concentration from 0 to 10 mg/L, and the order of Cd(II)-10 > Cd(II)-5 > Cd(II)-1 > Cd(II)-0 was achieved.

Different from Pb(II), the removal of Cr(VI) by activated carbon was inhibited by the presence of NOM. Only 79% of the equilibrium adsorption amount of Cr(VI)-0 was reached at 10 mg/L NOM in water, and the order of equilibrium adsorption amounts was Cr(VI)-0 > Cr(VI)-1 > Cr(VI)-5 > Cr(VI)-10. This should be attributed to the fact that the electronegativity of Cr(VI) (1.6) was less than that of Pb(II) (1.9), implying that Cr(VI) was less attractive to electrons than Pb(II) [39]. When the surface of activated carbon was



wrapped by NOM, it was difficult for Cr(VI) to be adsorbed by the anions of NOM. The amount of NOM encapsulated increased with raising NOM concentration, and the inhibitory effect of adsorption was also enhanced.

### 3.2.3. Adsorption thermodynamics under the influence of NOM

In order to evaluate the properties of activated carbon on the adsorption process of heavy metals and the effect of temperature on the adsorption effect, the thermodynamic tests of activated carbon on five heavy metals under the conditions of NOM of 0 and 10 mg/L were carried out. The thermodynamic parameters obtained are shown in Table 2.

The change process in the adsorption system can be inferred from the value of Gibbs free energy ( $\Delta G$ ). For the five heavy metals under all temperature conditions,  $\Delta G$  was negative, indicating that the adsorption reactions of activated carbon to Pb(II), Cu(II), Zn(II), Cd(II) and Cr(VI) were spontaneous process [35]. Moreover, the absolute value of  $\Delta G$  gradually increased with the increase of temperature. It

can be seen that higher reaction temperature was beneficial to the removal of heavy metals by activated carbon. In addition, the absolute values of  $\Delta G$  of Pb(II), Cu(II) and Cd(II) increased correspondingly when NOM existed in water, while the absolute value of  $\Delta G$  of Cr(VI) decreased correspondingly. Therefore, NOM was conducive to the spontaneous adsorption of Pb(II), Cu(II) and Cd(II), while inhibiting the spontaneous adsorption of Cr(VI), which was consistent with the results of adsorption kinetics. This was mainly due to the fact that a large number of functional groups were provided by NOM, and the coordination compounds of Pb(II)-NOM, Cu(II)-NOM and Cd(II)-NOM were produced, which promoted the spontaneous removal of heavy metals in the treatment system. The electronegativity of Cr(VI) was small, which meant that the ability to attract negative charges in NOM was weak, and some adsorption sites of activated carbon were occupied by NOM, resulting in a weakened spontaneous adsorption of Cr(VI) by activated carbon.

Whether the reaction process was endothermic or exothermic can be judged by the variation of enthalpy ( $\Delta H$ ). When the reaction system absorbed heat, the enthalpy value

Table 2  
Thermodynamic parameters comparison of adsorption for Pb(II), Cu(II), Zn(II), Cd(II) and Cr(VI) at NOM concentrations of 0 and 10 mg/L

Heavy metal	Temp. (°C)	NOM-0					NOM-10				
		$q_e$ (mmol/g)	$\Delta G$ (kJ/mol)	$\Delta H$ (kJ/mol)	$\Delta S$ (J/(mol K))	Adj- $R^2$	$q_e$ (mmol/g)	$\Delta G$ (kJ/mol)	$\Delta H$ (kJ/mol)	$\Delta S$ (J/(mol K))	Adj- $R^2$
Pb(II)	15	0.087	-12.701				0.111	-13.391			
	25	0.099	-13.531				0.124	-14.195			
	35	0.099	-13.985	6.844	67.992	0.926	0.124	-14.672	4.701	63.121	0.536
	45	0.111	-14.813	( $\sigma$ 0.955)	( $\sigma$ 3.111)		0.143	-15.640	( $\sigma$ 1.982)	( $\sigma$ 6.457)	
	55	0.118	-15.459				0.130	-15.800			
Cu(II)	15	0.112	-13.431				0.143	-14.165			
	25	0.144	-14.679				0.130	-14.364			
	35	0.128	-14.786	12.136	88.854	0.746	0.147	-15.234	6.005	69.372	0.396
	45	0.160	-16.032	( $\sigma$ 3.402)	( $\sigma$ 11.082)		0.179	-16.446	( $\sigma$ 3.155)	( $\sigma$ 10.276)	
	55	0.192	-17.228				0.163	-16.605			
Zn(II)	15	0.045	-10.953				0.042	-10.776			
	25	0.050	-11.616				0.055	-11.874			
	35	0.049	-11.950	8.953	68.804	0.823	0.053	-12.169	8.408	67.112	0.815
	45	0.059	-12.875	( $\sigma$ 2.020)	( $\sigma$ 6.568)		0.059	-12.875	( $\sigma$ 1.951)	( $\sigma$ 6.354)	
	55	0.070	-13.800				0.066	-13.620			
Cd(II)	15	0.034	-10.237				0.047	-11.066			
	25	0.041	-11.086				0.061	-12.157			
	35	0.048	-11.893	6.775	59.595	0.602	0.066	-12.789	9.238	71.191	0.806
	45	0.042	-11.898	( $\sigma$ 2.549)	( $\sigma$ 8.304)		0.074	-13.545	( $\sigma$ 2.202)	( $\sigma$ 7.172)	
	55	0.050	-12.786				0.072	-13.886			
Cr(VI)	15	0.160	-14.520				0.080	-12.480			
	25	0.161	-15.036				0.102	-13.559			
	35	0.183	-15.996	7.199	75.113	0.912	0.114	-14.307	8.619	74.025	0.557
	45	0.189	-16.647	( $\sigma$ 1.105)	( $\sigma$ 3.598)		0.130	-15.318	( $\sigma$ 3.513)	( $\sigma$ 11.440)	
	55	0.205	-17.481				0.116	-15.236			

Notes:  $q_e$  (mmol/g): adsorbed amount per activated carbon unit;  $\Delta G$  (kJ/mol): Gibbs free energy;  $\Delta H$  (kJ/mol): variation of enthalpy;  $\Delta S$  (J/(mol K)): variation of entropy; Adj- $R^2$ : adjusted determination coefficient;  $\sigma$ : standard deviation.

increased, and  $\Delta H$  was a positive value. When the reaction system emitted heat, the enthalpy value decreased, and  $\Delta H$  became a negative value [46,48]. It can be seen from Table 2 that the  $\Delta H$  values of Pb(II), Cu(II), Zn(II), Cd(II) and Cr(VI) were greater than 0, showing that the adsorption of metal ions on activated carbon was an endothermic process. After NOM was added to water, heat was required when the complex reaction between NOM and heavy metals occurred. This may be because the heavy metals were exchanged with the functional groups on the surface of activated carbon and NOM, and the process was generally endothermic. In addition, metal ions were adsorbed after losing hydration, and energy was needed in the process of ion dehydration. Thus, the removal of heavy metals was promoted by the increase in temperature, and the amount of adsorption by activated carbon was correspondingly increased.

The degree of chaos in the reaction system can be represented by entropy ( $S$ ). The greater the chaos of the system, the greater the  $S$  value. For Pb(II), Cu(II), Zn(II) and Cr(VI), the value of  $\Delta S$  decreased when NOM existed in water. It was speculated that metal ions could be more firmly adsorbed on the surface of NOM, and the randomness of solid-liquid interface was reduced. However, the  $\Delta S$  value of Cd(II) increased instead, confirming that Cd(II) had greater randomness in the coexistence system of activated carbon and NOM, which meant the recovery of Cd(II) may be hindered during the regeneration process [31]. In addition, the values of  $\Delta S$  in Table 2 were all greater than 0, implying the adsorption process of activated carbon for heavy metals was irreversible [45].

### 3.2.4. $N_2$ adsorption–desorption isotherm and pore-size distribution of the adsorbent

The adsorption capacity of activated carbon is mainly associated with the factors such as specific surface area, pore-size distribution and pore volume. The specific surface areas,  $N_2$  adsorption–desorption isotherms and pore-size distributions of the adsorbed activated carbon were determined, and the results are presented in Figs. 5 and 6.

Based on the IUPAC regulations [55],  $N_2$  adsorption–desorption isotherms are divided into six types, and their shapes depend on the pore structure of adsorbent. It can be observed from Fig. 5 that the adsorption curve of activated carbon used in the experiments had the characteristics of Type I and IV, confirming that the adsorbent was classified as a mixture of these two types. Type I isotherms indicate that the materials have micropores (pore size < 2 nm) [57,58], while Type IV isotherms imply that the materials are mainly mesopores (2 nm < pore size < 50 nm) [59]. Thus, most of the heavy metals in water were adsorbed by micropores and mesopores of activated carbon, which was demonstrated in the measurement of pore-size distributions. The large number of mesopores of activated carbon were conducive to the entry of large molecules of NOM, so that the influence of NOM on the removal of heavy metals was enhanced. Moreover, according to previous studies, it was known that metal ions, such as Pb(II), Cd(II) and Cr(VI), were more strongly adsorbed by activated carbon with a rich mesoporous structure. Additionally, the hysteresis loops of the isotherms were clearly observed at the relative pressure

of 0.75. This indicated that the activated carbon used in the experiments was monolayer chemisorption in the low-pressure region, and the metal ions were removed by the chemical bonds on the surface of the material. With the increase of relative pressure, the capillary condensations of activated carbon were occurred, and the physical adsorption of multi molecular layer appeared, which suggested that the adsorption reactions were dominated by van der Waals forces. According to the classification of IUPIC, these hysteresis loops belonged to Type H4, so that the layered structure of the adsorbent with slit-like pores was determined [60].

By comparing the  $N_2$  adsorption–desorption isotherms with NOM of 0 and 10 mg/L, the removal of Pb(II), Zn(II) and Cd(II) was promoted by the presence of NOM, while the adsorption of Cu(II) and Cr(VI) was inhibited under the same condition, which was consistent with the previous research conclusions.

As seen in Fig. 5c, the adsorption capacity of Zn(II) was significantly increased by NOM of 10 mg/L. The pore-size distributions showed that the microporous volume of activated carbon was increased when NOM was added. Further, the specific surface areas of the adsorbent under the conditions of Zn(II)-0 and Zn(II)-10 were 862 and 1,099  $m^2/g$  respectively, and the specific surface area of the material was also significantly increased by NOM. This may be due to the fact that NOM was loaded on the surface of activated carbon, which increased the surface pores of activated carbon, and NOM could also enter and be adsorbed in the macropores and mesopores of the particles, so that the larger pores were transformed into many micropores, thus increasing the microporous volume and specific surface area. Hence the adsorption performance of activated carbon was enhanced under the help of NOM.

Although the specific surface area of activated carbon was increased by NOM loading, the ionic radii of Pb(II) and Cd(II) were the largest among the five heavy metals, and the micropores of particles were easily blocked by Pb(II) and Cd(II) in the adsorption process, so the active sites could not be fully utilized. The little change of pore volumes in Fig. 6a and d was caused by both the promoting effect of NOM and the blocking effect of metal ions. Consequently, the adsorption capacity of activated carbon was slightly increased by NOM when the water was polluted by Pb(II) and Cd(II).

Among the five heavy metals, the electronegativity of Cu(II) was the largest, and the stability of the complex formed by the reaction of Cu(II) with NOM was also the strongest. The well-developed mesoporous material is conducive to the entry of macromolecular NOM. When NOM diffused into the particles, the ternary complex of activated carbon-Cu(II)-NOM was easy to be produced, which made a large amount of NOM accumulate in the material, and caused pore blockage and reduction of pore volume, thus the adsorption capacity of activated carbon was weakened [27]. This conjecture was confirmed by the decrease of adsorption quantity (Fig. 5b) and pore volume (Fig. 6b).

Because the ionic radius (0.52 Å) and electronegativity (1.6) of Cr(VI) were relatively small, and the complexation degree of Cr(VI) with NOM was weak, the pores in the adsorbent were not easily blocked by Cr(VI). Fig. 6e shows that the pore volumes of Cr(VI)-0 and Cr(VI)-10 were not much different, which should be interpreted as the function of

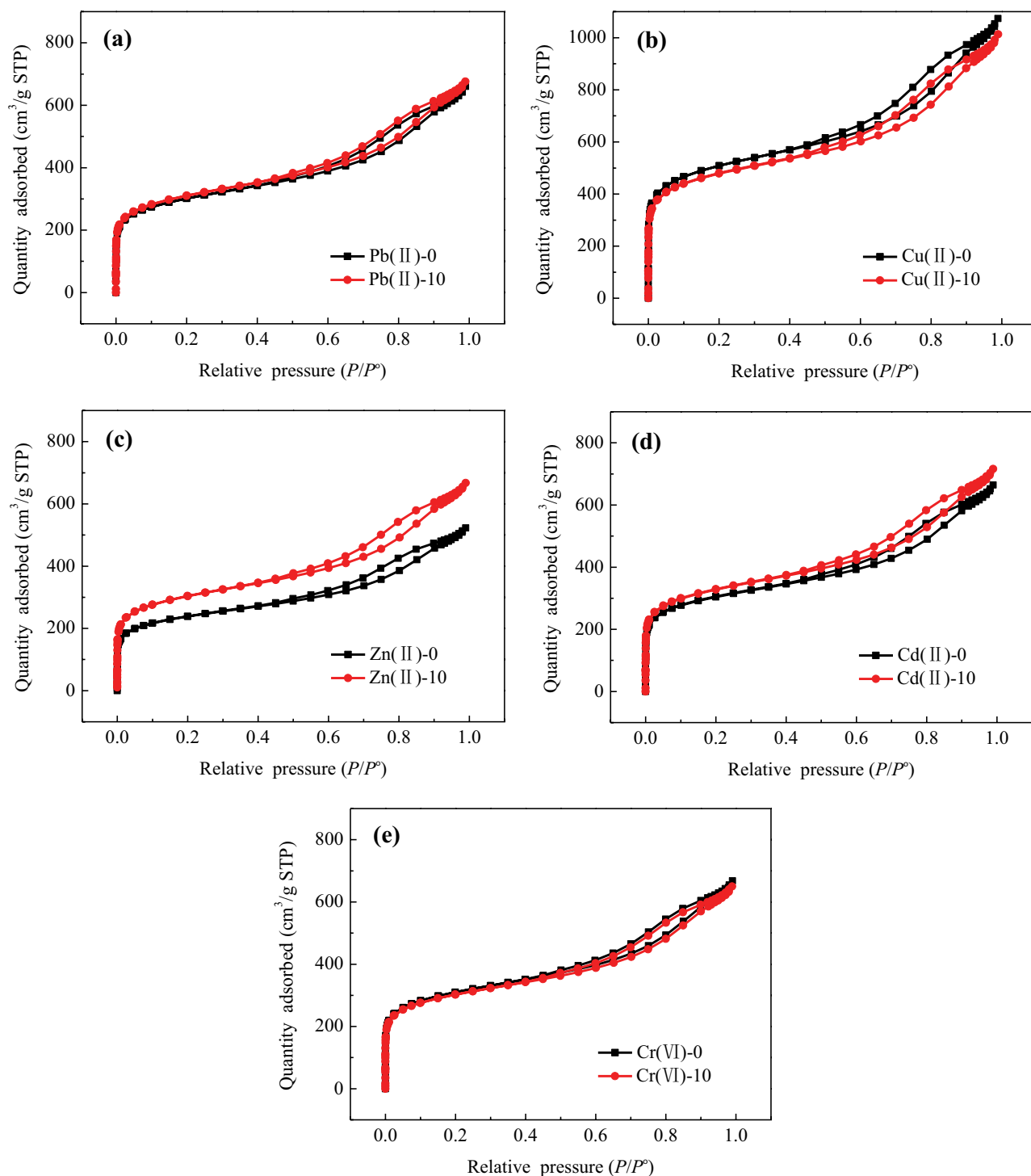


Fig. 5. N<sub>2</sub> adsorption–desorption isotherms of activated carbon for Pb(II), Cu(II), Zn(II), Cd(II) and Cr(VI).

NOM itself. NOM was attached to the surface of activated carbon and occupied part of the adsorption sites, but the new functional groups and specific surface area were also provided by NOM, so the specific surface areas and pore volumes of Cr(VI)-0 and Cr(VI)-10 were almost unchanged. Fig. 5e illustrates that the inhibition of NOM on the adsorption of heavy metals was only slight.

### 3.2.5. Surface morphology of the adsorbent

Surface morphology is a significant factor affecting the adsorption performance of material. The morphologies of activated carbon after adsorption of Pb(II), Cu(II), Zn(II), Cd(II) and Cr(VI) were observed by SEM. The results are shown in Fig. 7. It can be confirmed that the activated carbon

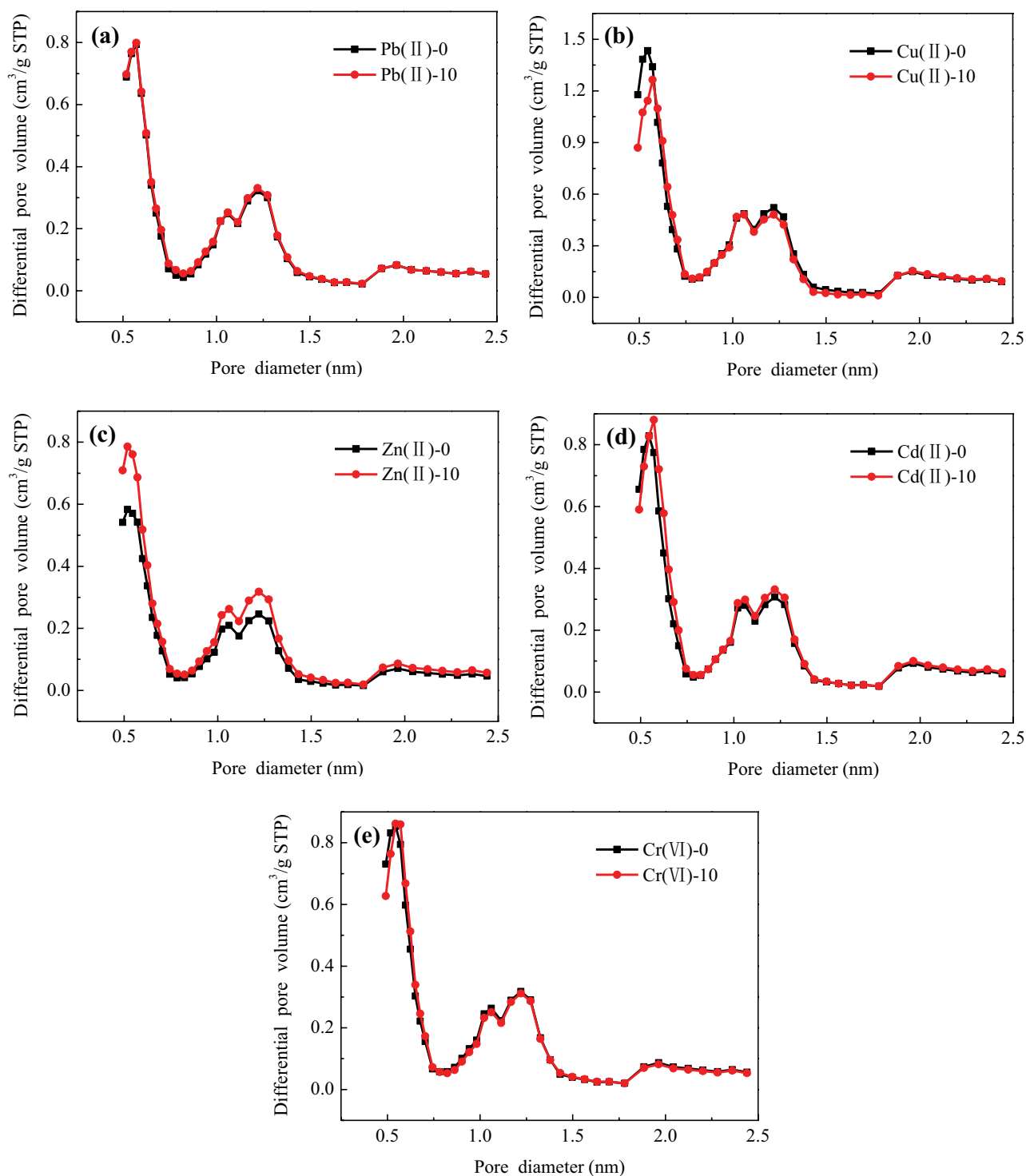


Fig. 6. Pore-size distributions of activated carbon for Pb(II), Cu(II), Zn(II), Cd(II) and Cr(VI).

used in the experiments was characterized by rough surface and many slit like pores. Some regions of activated carbon also had macroporous structure, which was connected with the interior of particles. Consequently, the specific surface area and pore volume of the adsorbent were increased.

As presented in Fig. 7a, there were many attachments on the surface of activated carbon, meaning that Pb(II)

was adsorbed on the active center in a large amount. Some elliptical macromolecular substances were found on the surface of the material in Fig. 7b, which may be NOM in water. The attachments on the surface of NOM were clearly observed, indicating that Pb(II) and NOM could be adsorbed by activated carbon, and new functional groups could also be provided by NOM, thereby forming activated

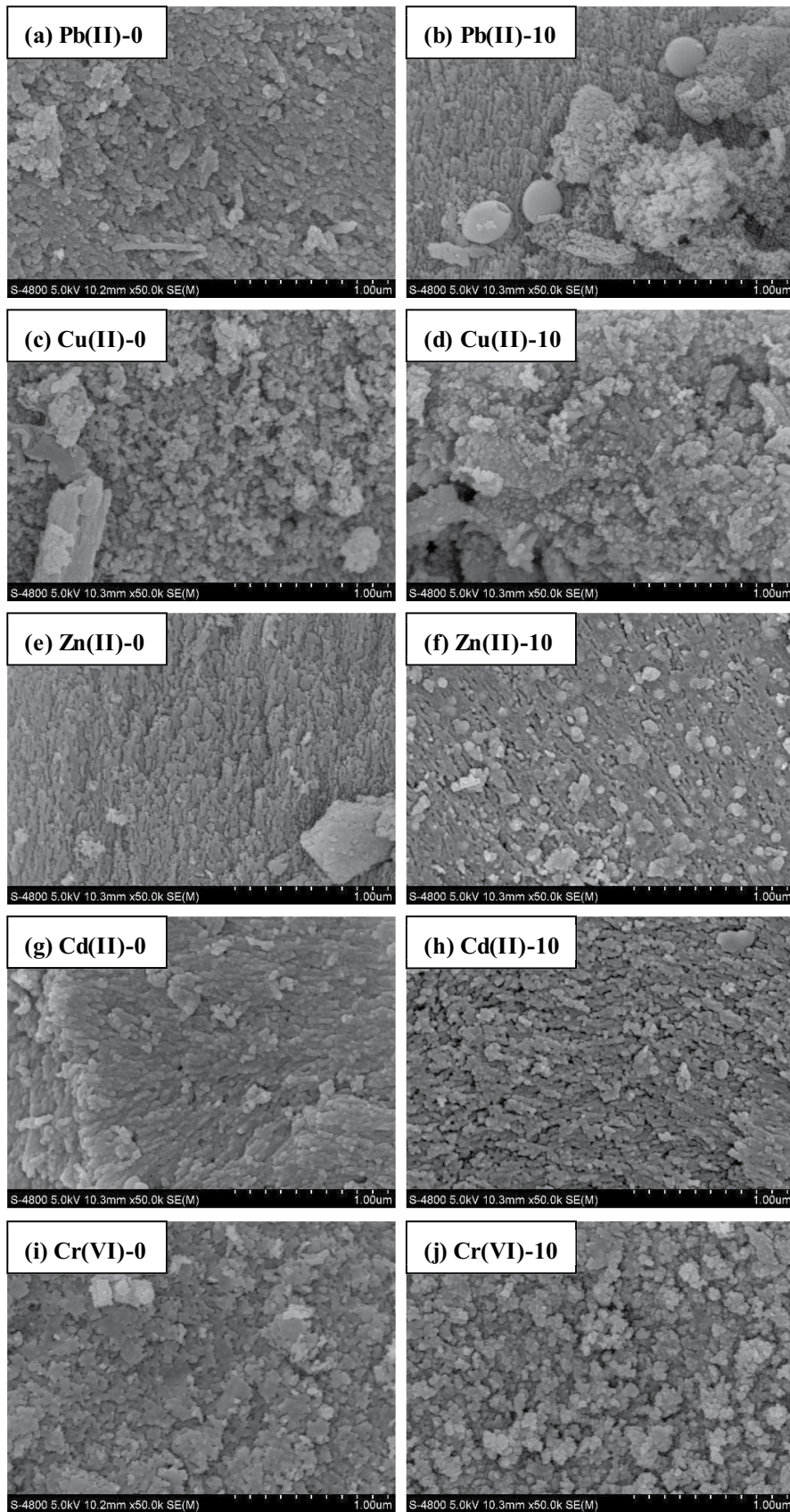


Fig. 7. SEM images of activated carbon after adsorption of Pb(II), Cu(II), Zn(II), Cd(II) and Cr(VI).



carbon-NOM-Pb(II) complexes. It was concluded that the adsorption of Pb(II) was promoted under the help of NOM, which confirmed the results of the previous study.

By comparing the morphologies of Zn(II)-0, Zn(II)-10, Cd(II)-0 and Cd(II)-10, it was found that the surface of the material was covered by a large number of oval NOM substances when high concentration of NOM was added. Since the precipitation reaction between Zn(II) and the hydroxyl groups in humic acid was prone to occur, and the affinity of Cd(II) with NOM was also strong, many Zn(II) and Cd(II) were adsorbed on the surface of NOM, and their removal efficiencies were also enhanced accordingly.

There were some irregular macroporous and mesoporous structures on the surface of activated carbon. As clearly seen in Fig. 7d and j, the polymer NOM could enter and block these pores, so that the adsorption space of the material was reduced, and the utilization of Cu(II) and Cr(VI) for the active sites in the particles was dramatically decreased. This led to the inhibitory effect of NOM on the removal of Cu(II) and Cr(VI).

### 3.3. Regeneration method of activated carbon

#### 3.3.1. Regeneration reagents

The desorption effects of H<sub>2</sub>O, NaCl, HCl and NaOH regeneration solutions on activated carbon for five heavy metals were investigated, and the results are shown in Fig. 8. The desorption rates of heavy metals were all less than 5% under the regeneration of deionized water H<sub>2</sub>O, while the desorption effects of NaCl and NaOH solutions were detected to be slightly better. HCl solution had the strongest desorption ability, and the desorption rates of Pb(II), Cu(II), Zn(II), Cd(II) and Cr(VI) could reach more than 85%. Based on the research, the desorption process of metal ions by H<sub>2</sub>O was controlled by physical action, such as van der Waals gravity. However, although physical adsorption had been proved to exist during the removal of heavy metals by activated carbon, chemical adsorption such as ion exchange and complexation reactions between functional groups on the surface of the material and heavy metals was the dominant

role [61,62]. This is the reason why the desorption rate of H<sub>2</sub>O was very low. The regeneration principles of activated carbon by NaCl and HCl solutions were basically the same. High concentration cations, such as Na<sup>+</sup> and H<sup>+</sup>, were used to replace the metal ions adsorbed on the surface of the material through competitive adsorption and ion exchange [63]. The desorption ability of HCl solution was stronger than that of NaCl solution, which was mainly attributed to the relative affinity between cations and adsorbent. It was reported that the relative affinity of H<sup>+</sup> to activated carbon was greater than that of Na<sup>+</sup>, and the higher the affinity, the stronger the power of ion exchange with heavy metals [64]. Besides, the ionic radius of H<sup>+</sup> was determined to be the smallest, and the mobility of H<sup>+</sup> in water was higher than that of Na<sup>+</sup>, which made metal ions easy to be contacted and exchanged by H<sup>+</sup>. The desorption rate of NaOH solution was only about 30%, which could be explained that NaOH is a strong alkaline solution. The protonation degree of the adsorbent could be weakened by NaOH, resulting in an increased attraction to metal ions, which was not conducive to the regeneration of activated carbon. Therefore, HCl solution had been proved to be the best regeneration reagent for desorption of metal ions from activated carbon.

#### 3.3.2. Regeneration reagent concentration

In order to determine the optimal concentration of regeneration reagent, the desorption experiments of activated carbon with adsorption equilibrium were conducted by modifying the concentrations of HCl solution from 0.01 to 1 mol/L, then heavy metals wastewater was treated with regenerated activated carbon. The results are shown in Fig. 9.

Fig. 9a illustrates that when the concentration of HCl solution increased from 0.01 to 0.2 mol/L, the desorption rates of five heavy metals were gradually increased to more than 91%, and the highest desorption rate of 97% for Pb(II) was achieved. But the desorption rate remained stable and was no longer raised as the concentration of HCl solution continued to increase. The reason for this phenomenon was that more H<sup>+</sup> in water was caused by the increase of HCl

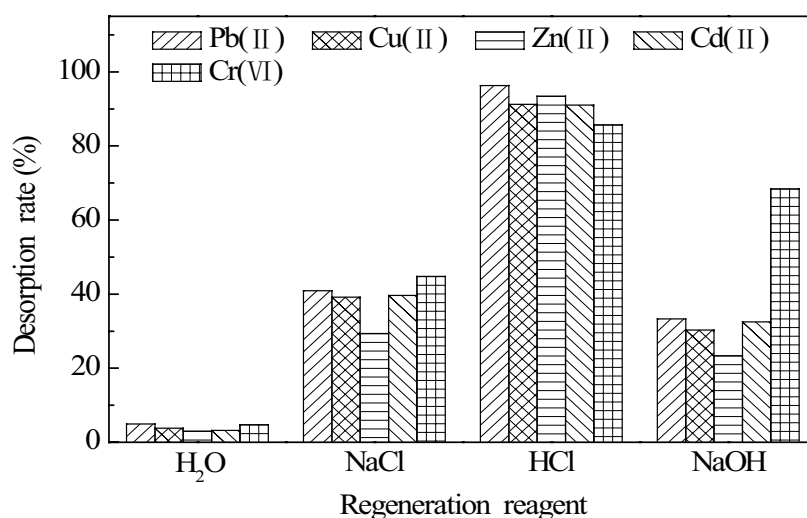


Fig. 8. Desorption capacities of different regeneration reagents for heavy metals on activated carbon.

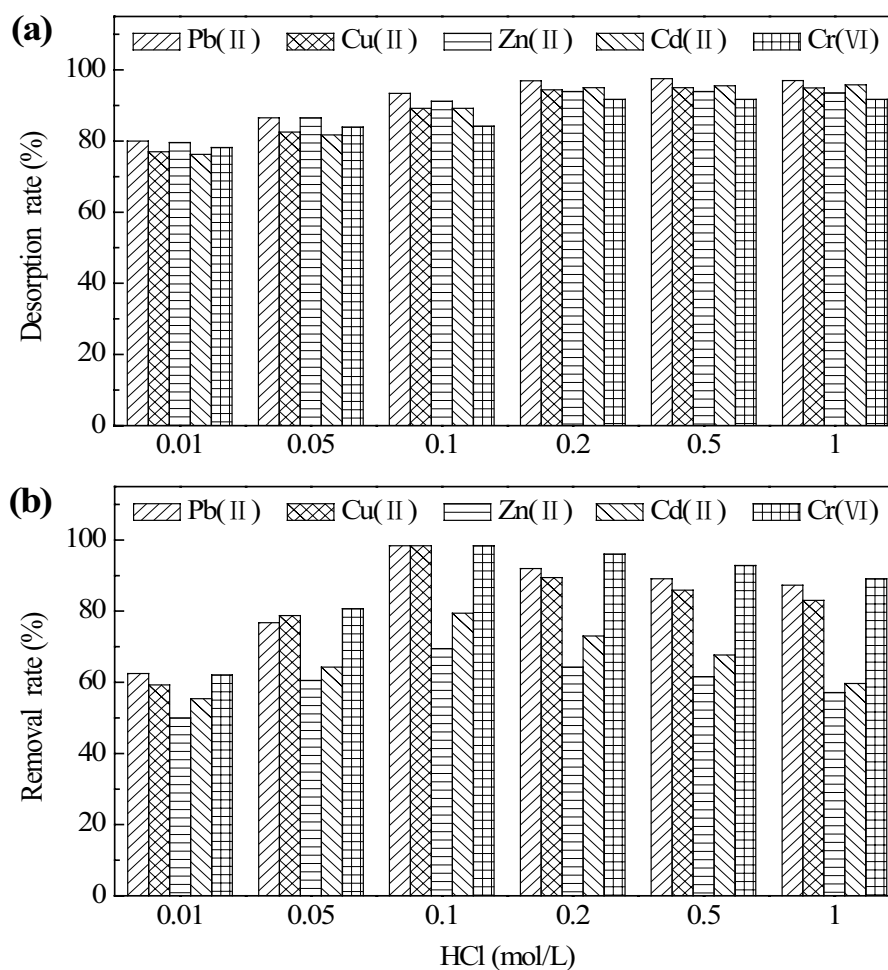


Fig. 9. Effect of HCl concentration on (a) desorption rates and (b) adsorption capacities of regenerated activated carbon.

concentration, and the ability of exchange with metal ions on the surface of activated carbon was correspondingly enhanced [63]. However, the desorption rate of 100% could not be obtained even if the concentration of HCl solution increased to a certain level. The strong chemical interaction was inferred to exist between metal ions and functional groups of activated carbon, such as internal surface chelation. The chemical bond was difficult to be broken by  $H^+$ , so the metal ions could not be replaced.

According to Fig. 9b, when the concentration of HCl solution was gradually increased to 0.1 mol/L, the adsorption capacities of regenerated activated carbon were significantly enhanced, and the removal rates of Pb(II), Cu(II) and Cr(VI) could be as high as 98%. But the removal efficiencies of five heavy metals decreased with the continuous increase the concentration of regeneration solution. This may be because as the concentration of HCl solution increased, the number of active centers occupied by  $H^+$  on the surface of activated carbon also raised, which was beneficial to the adsorption of metal ions after regeneration. However, HCl solution is strong acid, the surface morphology and structural characteristics of activated carbon would be destroyed by high concentration of HCl solution, and the adsorption performance would also be affected [65].

The optimal concentration of HCl solution was determined to be 0.1 mol/L through comprehensive analysis of the desorption rates of heavy metals and adsorption capacities of regenerated activated carbon.

### 3.3.3. Regeneration times

HCl solution of 0.1 mol/L was chosen to regenerate and reuse the adsorbed activated carbon for many times. Fig. 10 shows the role of regeneration times on the regeneration effect and adsorption performance of adsorbent.

As observed in Fig. 10a, after activated carbon had been used for six adsorption–regeneration cycles, the desorption effects of heavy metals by HCl solution were not varied from each other significantly, and the desorption rate was still as high as 80%, and even the desorption rate of Pb(II) could be maintained above 90%. This meant that activated carbon could be regenerated many times and the desorption effect was promising. Fig. 10b illustrates that the adsorption capacities of activated carbon for heavy metals were weakened with the increase of regeneration times, and the order of removal rates of Pb(II), Cu(II), Zn(II), Cd(II) and Cr(VI) was also changed, which was attributed to the oxidizing and corrosive properties of HCl. After many times of soaking



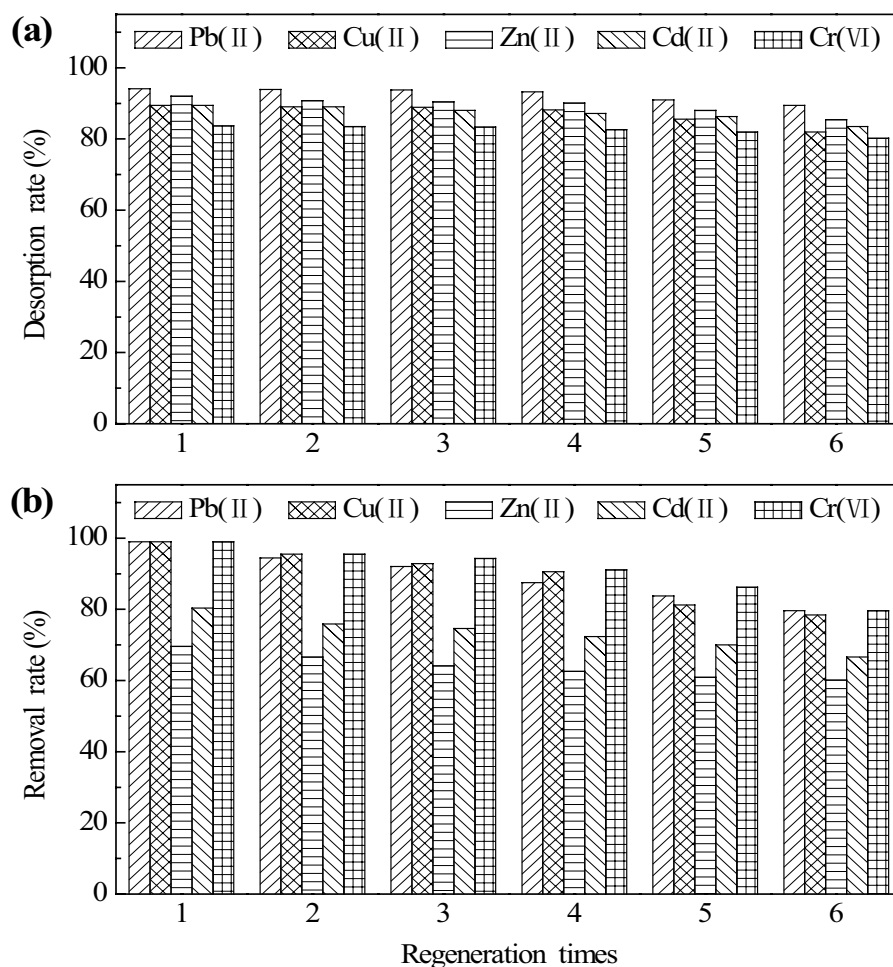


Fig. 10. Effect of regeneration times on (a) desorption rates and (b) adsorption capacities of regenerated activated carbon.

and desorption, some functional groups of activated carbon were easily oxidized, and the surface structure would be destroyed to some extent, and the internal pores of the particles would collapse, which resulted in the reduction of specific surface area and adsorption sites [65]. However, the removal rates of five heavy metals by activated carbon were all above 60% after the sixth regeneration, which suggested that the activated carbon could still be used normally after repeated regeneration [66].

All of these results demonstrated that activated carbon had good adsorption and regeneration performance, and could be recycled for more than six times, which greatly reduces the treatment cost and provides the possibility of economical and efficient treatment of heavy metal polluted wastewater.

#### 4. Conclusions

The adsorption capacities of activated carbon for different heavy metals were ranked as  $\text{Cu(II)} > \text{Cr(VI)} > \text{Pb(II)} > \text{Zn(II)} > \text{Cd(II)}$ , and the removal process was efficiently explained using the pseudo-second-order model. NOM, which is widely present in wastewater, could be loaded on activated carbon to increase the microporous volume and

specific surface area, and new functional groups were provided to form heavy metal-NOM coordination compounds. Therefore, the increases of equilibrium adsorption capacities of activated carbon for  $\text{Pb(II)}$ ,  $\text{Zn(II)}$ ,  $\text{Cd(II)}$  and  $\text{Cu(II)}$  were obtained under the help of 1 mg/L NOM. However, NOM contained a lot of polymer compounds, which easily caused the pores of activated carbon to be blocked and some of the adsorption sites to be occupied, and the electronegativity of  $\text{Cr(VI)}$  was proved to be small, which made it difficult for  $\text{Cr(VI)}$  to be adsorbed by the anions of NOM in large quantities. As a result, the equilibrium adsorption capacity of  $\text{Cr(VI)}$  was reduced with the addition of 1 mg/L NOM. Moreover, due to the combined action of the characteristics of five heavy metals, such as ionic radius, hydration heat, electronegativity and the stability of coordination compounds with NOM, different degrees of promoting or inhibiting effect for the adsorption of activated carbon could be caused by the different concentrations of NOM. The regeneration studies suggested that the metal ions on activated carbon were desorbed best by HCl solution of 0.1 mol/L, and activated carbon could be used for multiple adsorption–regeneration cycles, which is an economical and efficient adsorbent for heavy metals with good application prospects.

## Acknowledgments

This research was funded by the National Science and Technology Major Project of China (No. 2017ZX07107-005) and the Guangxi Major Projects of Science and Technology (No. GXMPST AA17202032). The experimental supporting by National Environmental and Energy Science and Technology International Cooperation Base in University of Science and Technology Beijing were greatly appreciated.

## References

- [1] G. Zhou, J. Luo, C. Liu, L. Chu, J. Crittenden, Efficient heavy metal removal from industrial melting effluent using fixed-bed process based on porous hydrogel adsorbents, *Water Res.*, 131 (2018) 246–254.
- [2] A. Celik, A. Demirbaş, Removal of heavy metal ions from aqueous solutions via adsorption onto modified lignin from pulping wastes, *Energy Sources*, 27 (2005) 1167–1177.
- [3] I. Kula, M. Uğurlu, H. Karaoğlu, A. Celik, Adsorption of Cd(II) ions from aqueous solutions using activated carbon prepared from olive stone by ZnCl<sub>2</sub> activation, *Bioresour. Technol.*, 99 (2008) 492–501.
- [4] S.L. Bazana, Q.L. Shimabuku-Biadola, F.S. Arakawa, R.G. Gomes, E.S. Cossich, R. Bergamasco, Modified activated carbon with silver-copper mixed oxides nanoparticles for removal of heavy metals from water, *Int. J. Environ. Sci. Technol.*, 16 (2019) 6727–6734.
- [5] Y. Song, L. Wang, B. Lv, G. Chang, W. Jiao, Y. Liu, Removal of trace Cr(VI) from aqueous solution by porous activated carbon balls supported by nanoscale zero-valent iron composites, *Environ. Sci. Pollut. Res.*, 27 (2020) 7015–7024.
- [6] T. Altun, H. Ecevit, Cr(VI) removal using Fe<sub>2</sub>O<sub>3</sub>-chitosan-cherry kernel shell pyrolytic charcoal composite beads, *Environ. Eng. Res.*, 25 (2020) 426–438.
- [7] R. Arora, Adsorption of heavy metals—a review, *Mater. Today: Proc.*, 18 (2019) 4745–4750.
- [8] F. Fu, Q. Wang, Removal of heavy metal ions from wastewaters: a review, *J. Environ. Manage.*, 92 (2011) 407–418.
- [9] C.F. Carolin, P.S. Kumar, A. Saravanan, G.J. Joshiba, M. Naushad, Efficient techniques for the removal of toxic heavy metals from aquatic environment: a review, *J. Environ. Chem. Eng.*, 5 (2017) 2782–2799.
- [10] C. Zhang, Y. Jiang, Y. Li, Z. Hu, L. Zhou, M. Zhou, Three-dimensional electrochemical process for wastewater treatment: a general review, *Chem. Eng. J.*, 228 (2013) 455–467.
- [11] V.K. Gupta, I. Ali, Removal of lead and chromium from wastewater using bagasse fly ash – a sugar industry waste, *J. Colloid Interface Sci.*, 271 (2004) 321–328.
- [12] Renu, M. Agarwal, K. Singh, Heavy metal removal from wastewater using various adsorbents: a review, *J. Water Reuse Desalin.*, 7 (2017) 387–419.
- [13] G. Issabayeva, M.K. Aroua, N.M.N. Sulaiman, Removal of lead from aqueous solutions on palm shell activated carbon, *Bioresour. Technol.*, 97 (2006) 2350–2355.
- [14] E.A. Deliyanni, G.Z. Kyzas, K.S. Triantafyllidis, K.A. Matis, Activated carbons for the removal of heavy metal ions: a systematic review of recent literature focused on lead and arsenic ions, *Open Chem.*, 13 (2015) 699–708.
- [15] S. Lo, S. Wang, M. Tsai, L. Lin, Adsorption capacity and removal efficiency of heavy metal ions by Moso and Ma bamboo activated carbons, *Chem. Eng. Res. Des.*, 90 (2012) 1397–1406.
- [16] W. Zheng, S. Chen, H. Liu, Y. Ma, W. Xu, Study of the modification mechanism of heavy metal ions adsorbed by biomass-activated carbon doped with a solid nitrogen source, *RSC Adv.*, 9 (2019) 37440–37449.
- [17] E. Koohzad, D. Jafari, H. Esmaili, Adsorption of lead and arsenic ions from aqueous solution by activated carbon prepared from *Tamarix* leaves, *ChemistrySelect*, 4 (2019) 12356–12367.
- [18] M. Wang, G. Bera, K. Mitra, T.L. Wade, A.H. Knap, T.D. Phillips, Tight sorption of arsenic, cadmium, mercury, and lead by edible activated carbon and acid-processed montmorillonite clay, *Environ. Sci. Pollut. Res.*, 28 (2021) 6758–6770.
- [19] E. Aboli, D. Jafari, H. Esmaili, Heavy metal ions (lead, cobalt, and nickel) biosorption from aqueous solution onto activated carbon prepared from *Citrus limetta* leaves, *Carbon Lett.*, 30 (2020) 683–698.
- [20] S.M. Kharrazi, N. Mirghaffari, M.M. Dastgerdi, M. Soleimani, A novel post-modification of powdered activated carbon prepared from lignocellulosic waste through thermal tension treatment to enhance the porosity and heavy metals adsorption, *Powder Technol.*, 366 (2020) 358–368.
- [21] J. Kyziol-Komosinska, I. Twardowska, A. Kocela, Adsorption of cadmium(II) ions from industrial wastewater by low moor peat occurring in the overburden of brown coal deposits, *Arch. Environ. Prot.*, 34 (2008) 83–94.
- [22] I. Levchuk, J.J.R. Márquez, M. Sillanpää, Removal of natural organic matter (NOM) from water by ion exchange – a review, *Chemosphere*, 192 (2018) 90–104.
- [23] Y. Matsui, D.R.U. Knappe, R. Takagi, Pesticide adsorption by granular activated carbon adsorbents. 1. Effect of natural organic matter preloading on removal rates and model simplification, *Environ. Sci. Technol.*, 36 (2002) 3426–3431.
- [24] W.-W. Tang, G.-M. Zeng, J.-L. Gong, J. Liang, P. Xu, C. Zhang, B.-B. Huang, Impact of humic/fulvic acid on the removal of heavy metals from aqueous solutions using nanomaterials: a review, *Sci. Total Environ.*, 468 (2014) 1014–1027.
- [25] S. Tuomikoski, R. Kupila, H. Romar, D. Bergna, T. Kangas, H. Runtti, U. Lassi, Zinc adsorption by activated carbon prepared from lignocellulosic waste biomass, *Appl. Sci.*, 9 (2019) 4583, doi: 10.3390/app9214583.
- [26] L. Dabek, Sorption of zinc ions from aqueous solutions on regenerated activated carbons, *J. Hazard. Mater.*, 101 (2003) 191–201.
- [27] E. Da'na, A. Awad, Regeneration of spent activated carbon obtained from home filtration system and applying it for heavy metals adsorption, *J. Environ. Chem. Eng.*, 5 (2017) 3091–3099.
- [28] S. Lata, P.K. Singh, S.R. Samadder, Regeneration of adsorbents and recovery of heavy metals: a review, *Int. J. Environ. Sci. Technol.*, 12 (2015) 1461–1478.
- [29] A. Larasati, G.D. Fowler, N.J.D. Graham, Insights into chemical regeneration of activated carbon for water treatment, *J. Environ. Chem. Eng.*, 9 (2021) 1–11.
- [30] C. Suo, K. Du, R. Yuan, H. Chen, F. Wang, B. Zhou, Adsorption study of heavy metal ions from aqueous solution by activated carbon in single and mixed system, *Desal. Water Treat.*, 183 (2020) 315–324.
- [31] J. Manfrin, A.C. Gonçalves Jr., D. Schwantes, E. Conradi Junior, J. Zimmermann, G.L. Ziemer, Development of biochar and activated carbon from cigarettes wastes and their applications in Pb<sup>2+</sup> adsorption, *J. Environ. Chem. Eng.*, 9 (2021) 104980, doi: 10.1016/j.jece.2020.104980.
- [32] J. Lin, L. Wang, Comparison between linear and non-linear forms of pseudo-first-order and pseudo-second-order adsorption kinetic models for the removal of methylene blue by activated carbon, *Front. Environ. Sci. Eng. China*, 3 (2009) 320–324.
- [33] R.M. Shrestha, I. Varga, J. Bajtai, M. Varga, Design of surface functionalization of waste material originated charcoals by an optimized chemical carbonization for the purpose of heavy metal removal from industrial waste waters, *Microchem. J.*, 108 (2013) 224–232.
- [34] D. Obregón-Valencia, M.D.R. Sun-Kou, Comparative cadmium adsorption study on activated carbon prepared from agave (*Mauritia flexuosa*) and olive fruit stones (*Olea europaea* L.), *J. Environ. Chem. Eng.*, 2 (2014) 2280–2288.
- [35] A.C. Gonçalves, D. Schwantes, M.A. Campagnolo, D.C. Dragunski, C.R.T. Tarley, A.K.D. Silva, Removal of toxic metals using endocarp of acai berry as biosorbent, *Water Sci. Technol.*, 77 (2018) 1547–1557.
- [36] S. Banerjee, S. Mukherjee, A. LaminKa-ot, S.R. Joshi, T. Mandal, G. Halder, Biosorptive uptake of Fe<sup>2+</sup>, Cu<sup>2+</sup> and As<sup>5+</sup> by activated biochar derived from *Colocasia esculenta*: isotherm, kinetics, thermodynamics, and cost estimation, *J. Adv. Res.*, 7 (2016) 597–610.

- [37] A.M. Youssef, T. El-Nabarawy, S.E. Samra, Sorption properties of chemically-activated carbons: 1. Sorption of cadmium(II) ions, *Colloids Surf., A*, 235 (2004) 153–163.
- [38] Z. Mahdi, Q.J. Yu, A.E. Hanandeh, Investigation of the kinetics and mechanisms of nickel and copper ions adsorption from aqueous solutions by date seed derived biochar, *J. Environ. Chem. Eng.*, 6 (2018) 1171–1181.
- [39] C. Faur-Brasquet, K. Kadirvelu, P.L. Cloirec, Removal of metal ions from aqueous solution by adsorption onto activated carbon cloths: adsorption competition with organic matter, *Carbon*, 40 (2002) 2387–2392.
- [40] A. Kuroki, M. Hiroto, Y. Urushihara, T. Horikawa, K.I. Sotowa, J.R. Alcántara Avila, Adsorption mechanism of metal ions on activated carbon, *Adsorption*, 25 (2019) 1251–1258.
- [41] K. Kadirvelu, C. Faur-Brasquet, P.L. Cloirec, Removal of Cu(II), Pb(II), and Ni(II) by adsorption onto activated carbon cloths, *Langmuir*, 16 (2000) 8404–8409.
- [42] S.J. Allen, P.A. Brown, Isotherm analyses for single component and multi-component metal sorption onto lignite, *J. Chem. Technol. Biotechnol. Biotechnol.*, 62 (2010) 17–24.
- [43] M.E. Zayat, E. Smith, Modeling of heavy metals removal from aqueous solution using activated carbon produced from cotton stalk, *Water Sci. Technol.*, 67 (2013) 1612–1619.
- [44] D. Schwantes, A.C. Goncalves, A. Schiller, J. Manfrin, A.G. Rosenberger, Eco-friendly, renewable *Crambe abyssinica* Hochst-based adsorbents remove high quantities of Zn<sup>2+</sup> in water, *J. Environ. Health Sci.*, 18 (2020) 809–823.
- [45] A.C. Goncalves, D. Schwantes, A.L. Braccini, F. Albornoz, E. Conradi, J. Zimmermann, Canola meal derived activated biochar treated with NaOH and CO<sub>2</sub> as an effective tool for Cd removal, *J. Chem. Technol. Biotechnol.*, 97 (2022) 87–100.
- [46] D. Schwantes, A.C. Goncalves, M.A. Campagnolo, C.R.T. Tarley, D.C. Dragunski, A. de Varennes, A.K.D. Silva, E. Conradi, Chemical modifications on pinus bark for adsorption of toxic metals, *J. Environ. Chem. Eng.*, 6 (2018) 1271–1278.
- [47] E. Conradi, A.C. Goncalves, D. Schwantes, J. Manfrin, A. Schiller, J. Zimmerman, G.J. Klassen, G.L. Ziemer, Development of renewable adsorbent from cigarettes for lead removal from water, *J. Environ. Chem. Eng.*, 7 (2019) 103200, doi: 10.1016/j.jece.2019.103200.
- [48] A.C. Goncalves, A.L. Braccini, D. Schwantes, M.A. Campagnolo, A.D. Schiller, J. Manfrin, E. Conradi, J. Zimmermann, Adsorbents developed from residual biomass of canola grains for the removal of lead from water, *Desal. Water Treat.*, 197 (2020) 261–279.
- [49] X. Liu, X. Xu, X. Dong, J. Park, Competitive adsorption of heavy metal ions from aqueous solutions onto activated carbon and agricultural waste materials, *Pol. J. Environ. Stud.*, 29 (2020) 749–761.
- [50] M. Touihri, S. Gouveia, F. Guesmi, C. Hannachi, B. Hamrouni, C. Cameselle, Low-cost biosorbents from pines wastes for heavy metals removal from wastewater: adsorption/desorption studies, *Desal. Water Treat.*, 225 (2021) 430–442.
- [51] M. Bilal, J. Ali, M.Y. Khan, R. Uddin, F. Kanwl, Synthesis and characterization of activated carbon from *Capparis decidua* for removal of Pb(II) from model aqueous solution: kinetic and thermodynamics approach, *Desal. Water Treat.*, 221 (2021) 185–196.
- [52] A. Pholosi, E.B. Naidoo, A.E. Ofomaja, Intraparticle diffusion of Cr(VI) through biomass and magnetite coated biomass: a comparative kinetic and diffusion study, *S. Afr. J. Chem. Eng.*, 32 (2020) 39–55.
- [53] H. Liu, S. Feng, N. Zhang, X. Du, Y. Liu, Removal of Cu(II) ions from aqueous solution by activated carbon impregnated with humic acid, *Front. Environ. Sci. Eng.*, 8 (2014) 329–336.
- [54] D.J. de Ridder, A.R.D. Verliefde, S.G.J. Heijman, J. Verberk, L.C. Rietveld, L.T.J. van der Aa, G.L. Amy, J.C. van Dijk, Influence of natural organic matter on equilibrium adsorption of neutral and charged pharmaceuticals onto activated carbon, *Water Sci. Technol.*, 63 (2011) 416–423.
- [55] A.L. Paredes-Doig, A. Pinedo-Flores, J. Aylas-Orejón, D. Obregon-Valencia, M.R.S. Kou, The interaction of metallic ions onto activated carbon surface using computational chemistry software, *Adsorpt. Sci. Technol.*, 38 (2020) 191–204.
- [56] D.P. Sountharajah, P. Loganathan, J. Kandasamy, S. Vigneswaran, Effects of humic acid and suspended solids on the removal of heavy metals from water by adsorption onto granular activated carbon, *Int. J. Environ. Res. Public Health*, 12 (2015) 10475–10489.
- [57] L. Dong, W. Liu, R. Jiang, Z. Wang, Study on the adsorption mechanism of activated carbon removing low concentrations of heavy metals, *Desal. Water Treat.*, 57 (2016) 7812–7822.
- [58] S. Alvarez-Torrellas, A. Rodriguez, G. Ovejero, J.M. Gomez, J. Garcia, Removal of caffeine from pharmaceutical wastewater by adsorption: influence of NOM, textural and chemical properties of the adsorbent, *Environ. Technol.*, 37 (2016) 1618–1630.
- [59] S.M. Kharrazi, M. Soleimani, M. Jokar, T. Richards, A. Pettersson, N. Mirghaffari, Pretreatment of lignocellulosic waste as a precursor for synthesis of high porous activated carbon and its application for Pb(II) and Cr(VI) adsorption from aqueous solutions, *Int. J. Biol. Macromol.*, 180 (2021) 299–310.
- [60] O. Üner, Ü. Geçgel, T. Avcu, Comparisons of activated carbons produced from sycamore balls, ripe black locust seed pods, and *Nerium oleander* fruits and also their H<sub>2</sub> storage studies, *Carbon Lett.*, 31 (2021) 75–92.
- [61] S.I. Eze, H.O. Abugu, L.C. Ekowo, Thermal and chemical pretreatment of *Cassia sieberiana* seed as biosorbent for Pb<sup>2+</sup> removal from aqueous solution, *Desal. Water Treat.*, 226 (2021) 223–241.
- [62] R. Shahrokh-Shahraki, C. Benally, M.G. El-Din, J. Park, High efficiency removal of heavy metals using tire-derived activated carbon vs. commercial activated carbon: insights into the adsorption mechanisms, *Chemosphere*, 264 (2021) 128455, doi: 10.1016/j.chemosphere.2020.128455.
- [63] M.M. Rao, A. Ramesh, G.P.C. Rao, K. Seshaiha, Removal of copper and cadmium from the aqueous solutions by activated carbon derived from *Ceiba pentandra* hulls, *J. Hazard. Mater.*, 129 (2006) 123–129.
- [64] M. Bilal, J.A. Shah, T. Ashfaq, S.M.H. Gardazi, A.A. Tahir, A. Pervez, H. Haroon, Q. Mahmood, Waste biomass adsorbents for copper removal from industrial wastewater—a review, *J. Hazard. Mater.*, 263 (2013) 322–333.
- [65] A. Larasati, G.D. Fowler, N.J.D. Graham, Insights into chemical regeneration of activated carbon for water treatment, *J. Environ. Chem. Eng.*, 9 (2021) 105555, doi: 10.1016/j.jece.2021.105555.
- [66] L. Zhou, Q. Yu, Y. Cui, F. Xie, W. Li, Y. Li, M. Chen, Adsorption properties of activated carbon from reed with a high adsorption capacity, *Ecol. Eng.*, 102 (2017) 443–450.

## Supporting information

Table S1  
Parameters comparison of adsorption kinetics for Pb(II) at different NOM concentrations

Sample	Pseudo-first-order				Pseudo-second-order		
	$q_{e(\text{exp.})}$ (mmol/g)	$q_{e(\text{cal.})}$ (mmol/g)	$k_1$ (1/min)	Adj- $R^2$	$q_{e(\text{cal.})}$ (mmol/g)	$k_2$ (g/(mmol min))	Adj- $R^2$
Pb(II)-0	0.099	0.093 ( $\sigma$ 0.002)	2.202 ( $\sigma$ 0.499)	0.970	0.095 ( $\sigma$ 0.002)	77.564 ( $\sigma$ 36.501)	0.974
Pb(II)-1	0.136	0.124 ( $\sigma$ 0.003)	2.967 ( $\sigma$ 1.254)	0.961	0.126 ( $\sigma$ 0.003)	70.164 ( $\sigma$ 41.985)	0.969
Pb(II)-5	0.127	0.118 ( $\sigma$ 0.002)	0.948 ( $\sigma$ 0.000)	0.964	0.122 ( $\sigma$ 0.002)	53.676 ( $\sigma$ 18.500)	0.983
Pb(II)-10	0.124	0.117 ( $\sigma$ 0.002)	1.346 ( $\sigma$ 0.000)	0.967	0.121 ( $\sigma$ 0.001)	48.659 ( $\sigma$ 11.618)	0.990

Sample	Intraparticle diffusion (Weber–Morris)						
	$k_i$ (mmol/(g min <sup>0.5</sup> ))		$d$ (mmol/g)		Adj- $R^2$		$D_i$ (cm <sup>2</sup> /s)
	Second phase	Third phase	Second phase	Third phase	Second phase	Third phase	
Pb(II)-0	0.010 ( $\sigma$ 0.006)	1.998e <sup>-4</sup> ( $\sigma$ 8.876e <sup>-5</sup> )	0.073 ( $\sigma$ 0.010)	0.093 ( $\sigma$ 7.939e <sup>-4</sup> )	0.378	0.448	7.558e <sup>-7</sup>
Pb(II)-1	7.024e <sup>-4</sup> ( $\sigma$ 3.534e <sup>-4</sup> )	4.332e <sup>-4</sup> ( $\sigma$ 4.650e <sup>-5</sup> )	0.116 ( $\sigma$ 0.001)	0.129 ( $\sigma$ 5.502e <sup>-4</sup> )	0.330	0.977	2.182e <sup>-7</sup>
Pb(II)-5	0.002 ( $\sigma$ 2.504e <sup>-4</sup> )	1.828e <sup>-4</sup> ( $\sigma$ 8.371e <sup>-5</sup> )	0.108 ( $\sigma$ 7.975e <sup>-4</sup> )	0.125 ( $\sigma$ 9.905e <sup>-4</sup> )	0.940	0.653	3.086e <sup>-7</sup>
Pb(II)-10	0.006 ( $\sigma$ 0.002)	3.471e <sup>-4</sup> ( $\sigma$ 1.642e <sup>-4</sup> )	0.101 ( $\sigma$ 0.004)	0.119 ( $\sigma$ 0.002)	0.699	0.464	3.779e <sup>-7</sup>

Notes:  $q_{e(\text{exp.})}$  and  $q_{e(\text{cal.})}$  (mmol/g): the  $q_e$  obtained by the experiment test and calculated by the model, respectively;  $k_1$  (1/min) and  $k_2$  (g/(mmol min)): the rate constants for pseudo-first-order and pseudo-second-order adsorption models, respectively;  $k_i$  (mmol/(g min<sup>0.5</sup>)): rate constant for intraparticle diffusion model;  $d$  (mmol/g): effect of boundary layer thickness;  $D_i$  (cm<sup>2</sup>/s): intraparticle diffusion coefficient; Adj- $R^2$ : adjusted determination coefficient;  $\sigma$ : standard deviation.

Table S2  
Parameters comparison of pseudo-second-order for Cu(II), Zn(II), Cd(II) and Cr(VI) at different NOM concentrations

Sample	Cu(II)				Sample	Zn(II)			
	$q_{e(\text{exp.})}$ (mmol/g)	$q_{e(\text{cal.})}$ (mmol/g)	$k_2$ (g/(mmol min))	Adj- $R^2$		$q_{e(\text{exp.})}$ (mmol/g)	$q_{e(\text{cal.})}$ (mmol/g)	$k_2$ (g/(mmol min))	Adj- $R^2$
Cu(II)-0	0.144	0.132 ( $\sigma$ 0.003)	26.568 ( $\sigma$ 8.381)	0.966	Zn(II)-0	0.056	0.054 ( $\sigma$ 7.411e <sup>-4</sup> )	79.282 ( $\sigma$ 17.298)	0.987
Cu(II)-1	0.153	0.144 ( $\sigma$ 0.003)	22.944 ( $\sigma$ 5.904)	0.976	Zn(II)-1	0.078	0.077 ( $\sigma$ 5.202e <sup>-4</sup> )	93.857 ( $\sigma$ 15.074)	0.997
Cu(II)-5	0.134	0.121 ( $\sigma$ 0.003)	34.060 ( $\sigma$ 12.813)	0.961	Zn(II)-5	0.066	0.062 ( $\sigma$ 9.649e <sup>-4</sup> )	134.589 ( $\sigma$ 55.985)	0.983
Cu(II)-10	0.131	0.118 ( $\sigma$ 0.003)	49.527 ( $\sigma$ 23.849)	0.961	Zn(II)-10	0.061	0.057 ( $\sigma$ 8.786e <sup>-4</sup> )	66.026 ( $\sigma$ 14.784)	0.984

Sample	Cd(II)				Sample	Cr(VI)			
	$q_{e(\text{exp.})}$ (mmol/g)	$q_{e(\text{cal.})}$ (mmol/g)	$k_2$ (g/(mmol min))	Adj- $R^2$		$q_{e(\text{exp.})}$ (mmol/g)	$q_{e(\text{cal.})}$ (mmol/g)	$k_2$ (g/(mmol min))	Adj- $R^2$
Cd(II)-0	0.041	0.040 ( $\sigma$ 5.556e <sup>-4</sup> )	211.916 ( $\sigma$ 79.764)	0.987	Cr(VI)-0	0.140	0.119 ( $\sigma$ 0.006)	6.867 ( $\sigma$ 2.309)	0.886
Cd(II)-1	0.045	0.041 ( $\sigma$ 0.001)	108.783 ( $\sigma$ 56.748)	0.936	Cr(VI)-1	0.113	0.099 ( $\sigma$ 0.004)	7.237 ( $\sigma$ 1.752)	0.937
Cd(II)-5	0.047	0.043 ( $\sigma$ 9.485e <sup>-4</sup> )	139.028 ( $\sigma$ 62.688)	0.967	Cr(VI)-5	0.101	0.096 ( $\sigma$ 0.004)	7.357 ( $\sigma$ 1.850)	0.931
Cd(II)-10	0.061	0.059 ( $\sigma$ 7.276e <sup>-4</sup> )	151.280 ( $\sigma$ 52.826)	0.989	Cr(VI)-10	0.097	0.094 ( $\sigma$ 0.003)	8.081 ( $\sigma$ 1.959)	0.937